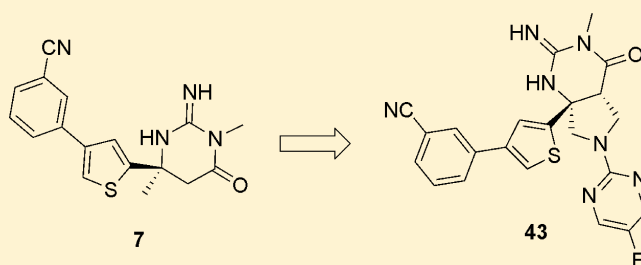


## Design and Validation of Bicyclic Iminopyrimidinones As Beta Amyloid Cleaving Enzyme-1 (BACE1) Inhibitors: Conformational Constraint to Favor a Bioactive Conformation

Mihirbaran Mandal,<sup>\*,†</sup> Zhaoning Zhu,<sup>†</sup> Jared N. Cumming,<sup>†</sup> Xiaoxiang Liu,<sup>†</sup> Corey Strickland,<sup>§</sup> Robert D. Mazzola,<sup>†</sup> John P. Caldwell,<sup>†</sup> Prescott Leach,<sup>‡</sup> Michael Grzelak,<sup>‡</sup> Lynn Hyde,<sup>‡</sup> Qi Zhang,<sup>‡</sup> Giuseppe Terracina,<sup>‡</sup> Lili Zhang,<sup>‡</sup> Xia Chen,<sup>‡</sup> Reshma Kuvelkar,<sup>‡</sup> Matthew E. Kennedy,<sup>‡</sup> Leonard Favreau,<sup>#</sup> Kathleen Cox,<sup>#</sup> Peter Orth,<sup>§</sup> Alexei Buevich,<sup>||</sup> Johannes Voigt,<sup>§</sup> Hongwu Wang,<sup>§</sup> Irina Kazakevich,<sup>⊥</sup> Brian A. McKittrick,<sup>†</sup> William Greenlee,<sup>†</sup> Eric M. Parker,<sup>‡</sup> and Andrew W. Stamford<sup>†</sup>

<sup>†</sup>Department of Medicinal Chemistry, <sup>‡</sup>Department of Neuroscience, <sup>§</sup>Global Structural Chemistry, <sup>||</sup>Department of Analytical Chemistry, <sup>⊥</sup>Department of Basic Pharmaceutical Sciences, and <sup>#</sup>Department of Exploratory Drug Metabolism, Merck Research Laboratories, 2015 Galloping Hill Road, Kenilworth, New Jersey 07033, United States

**ABSTRACT:** On the basis of our observation that the biaryl substituent of iminopyrimidinone **7** must be in a pseudoaxial conformation to occupy the contiguous S1–S3 subsites of BACE1, we have designed a novel fused bicyclic iminopyrimidinone scaffold intended to favor this bioactive conformation. Strategic incorporation of a nitrogen atom in the new constrained ring allowed us to develop SAR around the S2' binding pocket and ultimately resulted in analogues with low nanomolar potency for BACE1. In particular, optimization of the prime side substituent led to major improvements in potency by displacement of two conserved water molecules from a region near S2'. Further optimization of the pharmacokinetic properties of this fused pyrrolidine series, in conjunction with facile access to a rat pharmacodynamic model, led to identification of compound **43**, which is an orally active, brain penetrant inhibitor that reduces  $A\beta_{40}$  in the plasma, CSF, and cortex of rats in a dose-dependent manner.



## INTRODUCTION

Notwithstanding enormous progress made in science and medicine around Alzheimer's disease (AD), a treatment to slow or halt the progression of this devastating illness is still out of reach. To date, the only therapies available for AD patients are cholinesterase inhibitors such as donepezil and the NMDA receptor antagonist memantine.<sup>1</sup> With the emergence of the amyloid hypothesis based on discoveries using biochemistry, human genetics, and pathology,<sup>2</sup> vigorous research in both academia and industry was undertaken to address this unmet medical need. The presence of  $\beta$ -amyloid plaques and neurofibrillary tangles of tau protein in the brain are key hallmarks of AD. The plaques are mainly composed of fibrillar aggregates of insoluble  $\beta$ -amyloid peptides ( $A\beta_{40,42}$ ), and it is now recognized that the soluble, lower molecular weight oligomers of  $A\beta_{40,42}$  are also key culprits contributing to the cognitive decline in Alzheimer's patients.<sup>3</sup> The  $A\beta_{40,42}$  peptides are generated from intraneuronal amyloid precursor protein (APP) through sequential cleavage by  $\beta$ -secretase (BACE1) and by  $\gamma$ -secretase, and thus agents that inhibit these enzymes would be beneficial as disease modifying treatments for AD. Indeed, human genetic mutations such as the Swedish mutation lead to enhanced  $\beta$ -secretase processing of APP, excess CNS  $A\beta$  levels, and ultimately aggressive early onset AD, under-

scoring the critical role of  $A\beta$  in AD.<sup>4</sup> While the approach of  $\gamma$ -secretase inhibition had appeared promising, progression through the clinic has been hampered by mechanism-based side effects largely mediated by concomitant inhibition of Notch processing.<sup>5</sup> On the other hand,  $A\beta$  lowering through inhibition of BACE1<sup>6</sup> represents an excellent alternative therapeutic strategy because BACE1 knockout mice show complete absence of  $A\beta$  production coupled with relatively moderate phenotypes.<sup>7,8</sup> Furthermore, crossing BACE1 knockout mice with PDAPP mice, which overproduce a mutant form of human APP, reversed the synaptic deficits and neurodegenerative pathologies characteristic of AD in the resulting biogenic mice.<sup>9,10</sup> From these studies, only a moderate reduction of CNS  $A\beta$  observed in BACE1 heterozygous/PDAPP mice resulted in significantly less plaque accumulation over time. These data suggest that inhibition of BACE1 could be an excellent strategy for the treatment and prevention of AD by providing potent inhibition of  $A\beta$  peptide formation in

**Special Issue:** Alzheimer's Disease

**Received:** July 16, 2012

**Published:** September 18, 2012

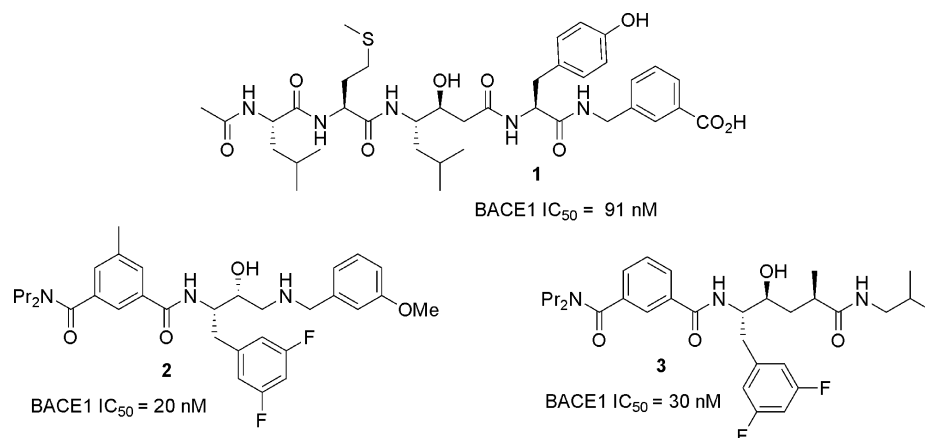


**Figure 1.** Potent peptidomimetic BACE1 inhibitors.

combination with the anticipation of an acceptable tolerability profile.

BACE1 is a membrane bound aspartyl protease expressed in the CNS. Early BACE1 inhibitor designs were inspired by the success of transition state mimetics in other drug targets from the aspartyl protease family such as HIV protease and renin.<sup>11,12</sup> Following that approach, Ghosh and Tang were the first to report on potent peptidic inhibitors including several crystal structures of these potent ligands complexed with BACE1.<sup>13</sup> Subsequent efforts produced many potent inhibitors containing statine (cf. **1**),<sup>14</sup> hydroxyethylene (cf. **2**),<sup>15</sup> and hydroxyethyl amine (cf. **3**)<sup>16</sup> cores (Figure 1). However, unlike HIV protease and renin, BACE1 is not a peripheral target. The high molecular weight, low permeability, and high susceptibility to P-glycoprotein (P-gp) efflux of these peptidomimetics made them unsuitable for further development as brain penetrant drugs.<sup>17</sup>

In parallel with the peptidomimetic approach, we and others<sup>18,19</sup> pursued fragment-based lead generation (FBLG) strategies to identify lower molecular weight (<300 Da) leads. From our FBLG efforts, HSQC screening using <sup>15</sup>N-BACE1,<sup>18</sup> we identified isothioureia **4** as a weak inhibitor of BACE1 that, based on NMR chemical shift perturbations, had interactions with both aspartic acids of the catalytic dyad as well as with other residues in the S1 and S3 subsites of BACE1. The X-ray cocrystal structure of this fragment with BACE1 showed that the amidine portion of isothioureia **4** formed a network of interactions with the catalytic aspartic acids by displacing a conserved water molecule. Recently, we have described the progression of **4** to a potent iminohydantoin **5** as a part of an affinity-driven optimization campaign (Figure 2).<sup>18</sup> Subsequently, with a focus on ligand efficiency, improved oral bioavailability, and improved selectivity, we developed a highly optimized iminohydantoin inhibitor **6**<sup>20</sup> and discovered a structurally distinct chemical series, the iminopyrimidinones, represented by compound **7**.<sup>21</sup> These structure-based design efforts led to the discovery of the first orally available brain penetrant small molecule BACE1 inhibitors.

To further improve the potency of iminopyrimidinone series, we have now designed a bicyclic iminopyrimidinone core to introduce conformational constraint and to facilitate access to the prime side of the BACE1 active site. Details of the structure–activity relationships (SAR) of prime side substitution, including discovery of a new binding pocket, will be reported in this article. Ultimately, structure-based evolution of

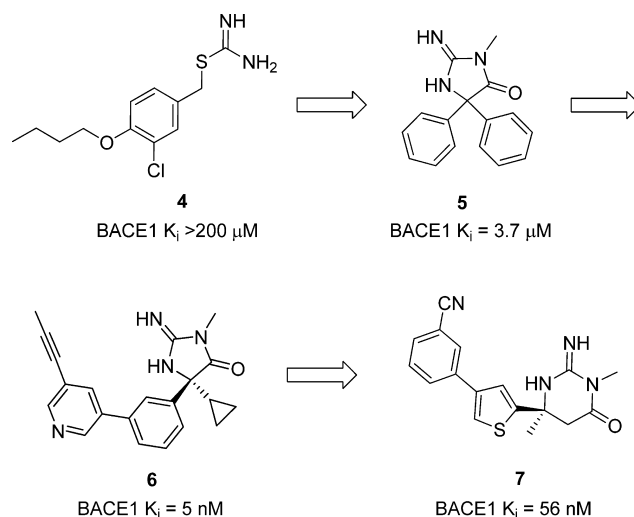


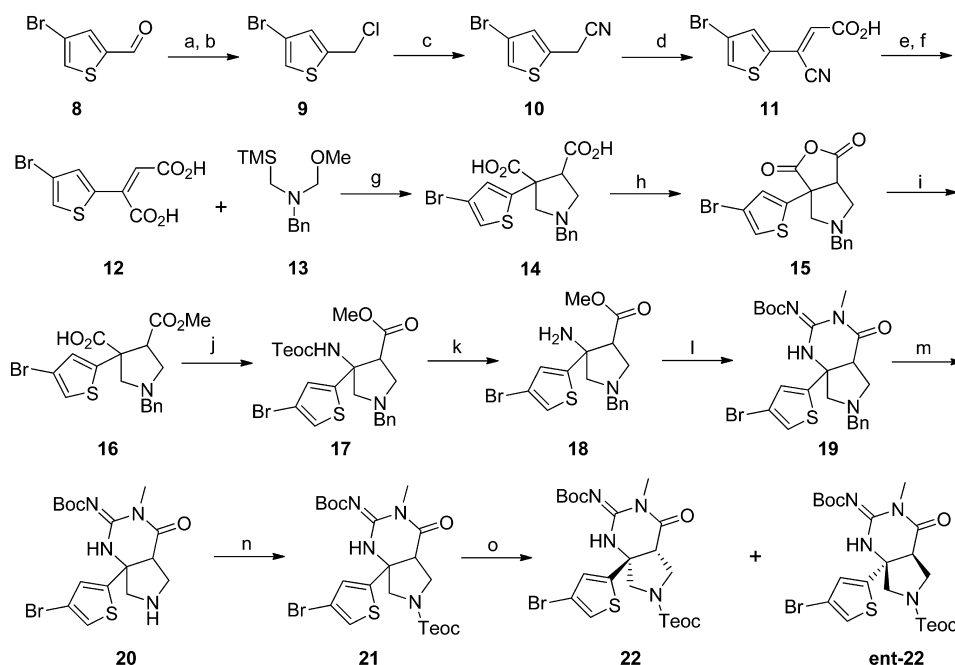
**Figure 2.** Evolution of iminopyrimidinone **7** through iminohydantoin **5** and **6** from the FBLG lead **4**.

this novel bicyclic series resulted in discovery of the potent, centrally efficacious lead compound **43**.

## CHEMISTRY

The synthesis of key intermediate **22** is depicted in Scheme 1. Commercially available 4-bromothiophene-2-carbaldehyde **8** was reduced by sodium borohydride, and the corresponding alcohol was converted to 4-bromo-2-(chloromethyl)thiophene **9** using thionyl chloride. Conversion of chloride **9** to the corresponding cyanide **10** was complicated due to the likely formation of condensed products from the reaction of product with the starting material. After evaluation of several reaction conditions, we found that oven-dried potassium cyanide was critical to minimize the formation of these side products. Once obtained, the 2-(4-bromothiophen-2-yl)acetonitrile **10** was condensed with glyoxalic acid, and product **11** precipitated from the reaction mixture.<sup>22</sup> Refluxing compound **11** in a mixture of sulfuric and formic acid hydrolyzed the nitrile and formed an intermediate anhydride that itself was hydrolyzed to diacid **12**. Formation of the key pyrrolidine ring was mediated through a [2 + 3] cycloaddition reaction between compound **12** and the dipolarophile *N*-benzyl-1-methoxy-*N*-((trimethylsilyl)methyl)-methanamine **13**. The resulting product **14** was then treated directly without purification with acetic

**Scheme 1. Synthesis of (4*R*,7*aR*)-2-(Trimethylsilyl)ethyl 7*a*-(4-Bromothiophen-2-yl)-2-((*tert*-butoxycarbonyl)imino)-3-methyl-4-oxohexahydro-1*H*-pyrrolo[3,4-*d*]pyrimidine-6(2*H*)-carboxylate **22**, Key Intermediate for SAR Studies<sup>a</sup>**



<sup>a</sup>Reagents and conditions: (a) NaBH<sub>4</sub>, MeOH, 0 °C; (b) SOCl<sub>2</sub>, CH<sub>2</sub>Cl<sub>2</sub>, room temperature (rt); (c) KCN, acetonitrile, reflux; (d) 50% glyoxylic acid in water, K<sub>2</sub>CO<sub>3</sub>, MeOH, rt; (e) 10% concentrated H<sub>2</sub>SO<sub>4</sub> in formic acid, 100 °C; (f) water, acetonitrile, 40 °C; (g) THF, 0 °C; (h) acetic anhydride, 90 °C; (i) MeOH, 0 °C; (j) diphenyl phosphorazidate, Et<sub>3</sub>N, toluene, then TMS-ethanol, 120 °C; (k) 4N HCl in dioxane, rt; (l) *t*-butyl *N*-[(methylamino)thioxomethyl]carbamate, EDCl, DIEA, DMF, rt; (m) chloroethyl chloroformate, K<sub>2</sub>CO<sub>3</sub>, dichloromethane, rt; (n) 2,5-dioxopyrrolidin-1-yl 2-(trimethylsilyl)ethyl carbonate, Et<sub>3</sub>N, dichloromethane, rt; (o) chiral HPLC (details in Experimental Section).

**Table 1. Selected SAR of Amides**

cpd	R <sup>1</sup>	R <sup>2</sup>	MW (ClogP)	BACE1 K <sub>i</sub> (nM) <sup>a</sup>	HEK293 IC <sub>50</sub> (nM) <sup>a</sup>	LE	CatD/BACE1 <sup>b</sup>	Rat AUC <sub>0-6h</sub> (μM.hr) <sup>c</sup>
26		H	455 (2.8)	3	19	0.36	64	0.024
27		F	491 (3.1)	2	20	0.34	34	0.30
28		F	488 (2.9)	1	8	0.35	56	0.30

<sup>a</sup>BACE1 K<sub>i</sub> and cell IC<sub>50</sub> values are the average of a minimum of two independent determinations. <sup>b</sup>Selectivity ratios were derived from cathepsin-D K<sub>i</sub> values (average of a minimum of two independent determinations). <sup>c</sup>Oral dose 10 mg/kg.

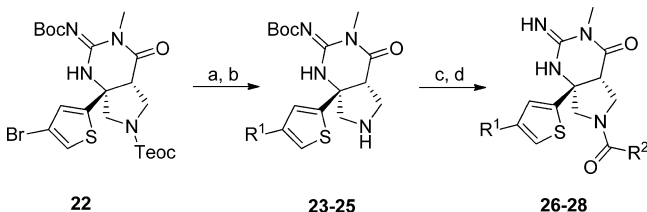
anhydride to reform an anhydride **15**. This anhydride underwent solvolysis with methanol at the less hindered center to give compound **16** with excellent regioselectivity. This monoacid was converted to protected amine **17** by a Curtius rearrangement followed by treatment with 2-(trimethylsilyl)ethanol, and the amine functionality was subsequently unmasked by treatment with HCl to provide compound **18**. Coupling of this material with *t*-butyl *N*-[(methylamino)thioxomethyl]-carbamate using standard peptide coupling

conditions followed by in situ intramolecular ring closure provided protected racemic iminopyrimidinone **19**. To facilitate downstream resolution of the enantiomers, the benzyl protecting group of compound **19** was swapped for a Teoc protecting group. Thus, treatment of compound **19** with chloromethyl chloroformate produced free amine **20** that was reprotected using *N*-[2-(trimethylsilyl)ethoxycarbonyloxy]-succinimide (Teoc-OSu) to provide penultimate intermediate **21**. The enantiomers of compound **21** were separated on

multihundred gram scale using chiral HPLC to provide desired isomer **22** and its enantiomer ent-**22**.

The amides shown in Table 1 were synthesized through the reaction sequence described in Scheme 2. Suzuki reactions

### Scheme 2. Synthesis of Amides 26–28<sup>a</sup>



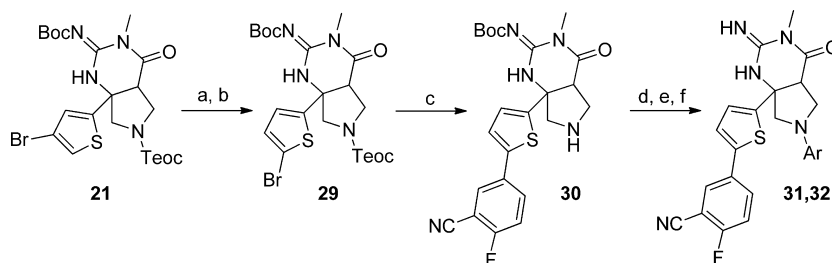
<sup>a</sup>Reagents and conditions: (a) R<sup>1</sup>-boronic acid, dichloro[1,1'-bis(diphenylphosphino)ferrocene]-palladium(II) dichloromethane, *tert*-butanol, K<sub>2</sub>CO<sub>3</sub>, 60 °C; (b) TBAF, THF, 0 °C; (c) R<sup>2</sup>-CO<sub>2</sub>H, EDCl, HOBT, DIEA, dichloromethane, rt; (d) trifluoroacetic acid, dichloromethane, rt.

between bromide **22** and various boronic acids installed the biaryl moiety, and subsequent treatment of the products with TBAF resulted in Teoc removal from the pyrrolidine nitrogen. Coupling of these free amines (compounds **23–25**) with various acids followed by treatment of the resulting compounds with TFA provided analogues **26–28**.

As shown in Scheme 3, the 2,5-thiophene isomer could be accessed easily from the same advanced intermediate as the 2,4-thiophene isomers above. To that end, debromination of compound **21** followed by treatment of the resulting compound with NBS installed the bromide in the 5 position of the thiophene. Following similar protocols as those described above for biaryl formation and pyrrolidine deprotection, compound **29** was converted to free amine **30**. In this case, the free pyrrolidine core was subjected to palladium-mediated arylation that, following removal of the Boc protecting group, provided analogues **31** and **32**.

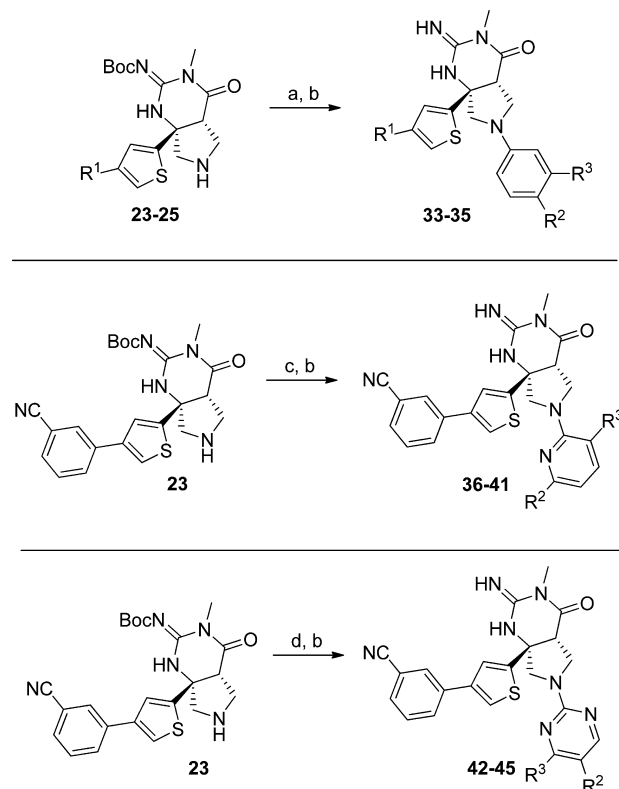
The remainder of the analogues discussed in this manuscript were synthesized from intermediates **23–25** using a variety of *N*-arylation conditions (Scheme 4) followed by TFA-mediated deprotection of the core. Compounds **33–35** were obtained through copper acetate mediated coupling with an appropriate boronic acid.<sup>23</sup> On the other hand, compounds **36–45** were made with palladium mediated *N*-arylation chemistry<sup>24</sup> using the appropriate pyridine or pyrimidine halide.

### Scheme 3. Synthesis of *N*-Phenyl Analogue in the 2,5-Thiophene Series (**31**, **32**)<sup>a</sup>



<sup>a</sup>Reagents and conditions: (a) 10% Pd/C, H<sub>2</sub>, methanol, rt; (b) NBS, DMF, rt; (c), (3-cyano-4-fluorophenyl)boronic acid, dichloro[1,1'-bis(diphenylphosphino)ferrocene]palladium(II) dichloromethane, *tert*-butanol, K<sub>2</sub>CO<sub>3</sub>, 60 °C; (d) TBAF, THF, 0 °C; (e) Tris-(dibenzylideneacetone)dipalladium, tri-*t*-butylphosphonium tetrafluoroborate, toluene, ArBr, NaOt-Bu, 80 °C; (f) trifluoroacetic acid, dichloromethane, rt.

### Scheme 4. Synthesis of Compounds 36–45<sup>a</sup>



<sup>a</sup>Reagents and conditions: (a) aryl boronic acid, Cu(OAc)<sub>2</sub>, Et<sub>3</sub>N, dichloromethane, rt; (b) TFA in dichloromethane, rt; (c) 2-bromo-substituted pyridine, Tris(dibenzylideneacetone)dipalladium(0), racemic-2,2'-bis-(diphenylphosphino)-1,1'-binaphthyl, NaOt-Bu, 80 °C; (d) 2-halo-substituted pyrimidine, palladium acetate, 2'-(di-*tert*-butylphosphino)-*N,N*-dimethylbiphenyl-2-amine, NaOt-Bu, 80 °C.

## RESULTS AND DISCUSSION

The X-ray cocrystal structure of iminopyrimidinone **7**<sup>21</sup> bound to BACE1 showed that the biaryl substituent is oriented in a pseudoaxial conformation to occupy the continuous S1–S3 hydrophobic pocket. In an attempt to bias the energetics of the molecule toward this active conformer, a C5–C6 cycle (cf. **7a**) was predicted to stabilize the pseudoaxial conformation by 0.92 kcal/mol (Figure 3). In addition, modeling indicated that substitution of the new fused ring structures would provide access to space in or near the S2' pocket. On the basis of these



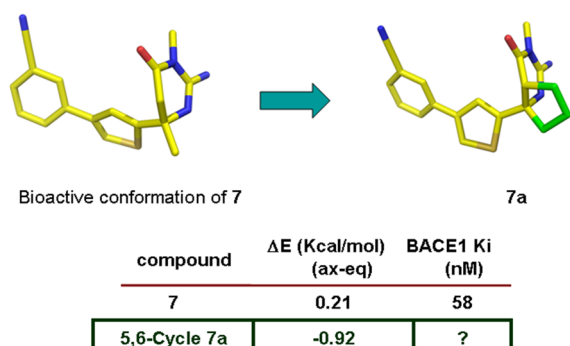


Figure 3. Conformational analysis.

computational results, development of a bicyclic version of 7 became a high priority.

Modeling of possible rings to fuse to the C5–C6 position of the iminopyrimidinone core suggested that a 3,4-fused pyrrolidine would provide the optimal trajectory for substituents on the nitrogen to reach the S2' subsite. Overlay of a model of benzamide 26 with the X-ray structure of compound 7 revealed the likelihood that the carbonyl oxygen of the benzamide would perturb or even displace one of the three conserved water molecules due to their close proximity (Figure 4a). Because these water molecules form a hydrogen bonding network among Trp<sup>76</sup>, Asn<sup>37</sup>, Ile<sup>126</sup>, Ser<sup>35</sup>, and Asp<sup>32</sup> in the protein surface (Figure 4b), the potential impact of disturbing one such conserved water molecule was unclear. In fact, upon synthesis, compound 26 showed a 19-fold improvement of potency (BACE1  $K_i$  = 2.0 nM) over compound 7.

The X-ray crystal structure of compound 26 bound to BACE1 (Figure 5) showed that the core and biaryl substituent bind in a similar fashion as was observed for the nonfused iminopyrimidinones (e.g., 7). Additionally, none of the three conserved water molecules adjacent to the S2' binding pocket were actually displaced but instead were reorganized to accommodate the new benzamide substituent. The water molecule that was nearest (1.1 Å) the amide oxygen of compound 26 in docking studies was perturbed by 1.8 Å from its original position to maintain the hydrogen bonding network observed with compound 7. From its new position, this water

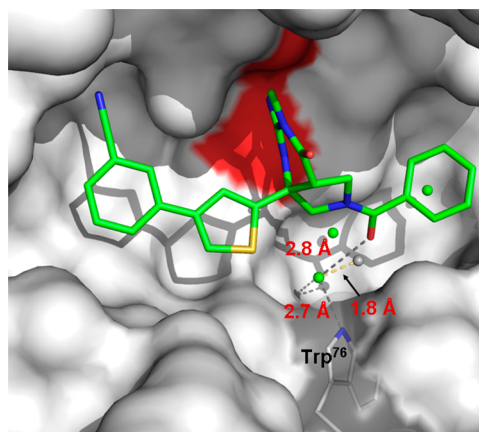


Figure 5. Co-crystal structure of 26 (green, PDB ID code: 4H1E) with BACE1 (catalytic dyad in red). One of the three water molecules moved 1.8 Å away from its original position (gray sphere) to reside 2.8 Å away from the amide carbonyl and 2.7 Å away from the NH of Trp<sup>76</sup>.

molecule was also within hydrogen bonding distance (2.8 Å) of the amide oxygen of 26 (Figure 5).

The significant improvement in affinity for this first bicyclic iminopyrimidinone 26 established this fused pyrrolidine series as an alternative BACE1 inhibitor scaffold. The compound was very potent in the cell-based assay, with an  $\alpha\beta$  IC<sub>50</sub> of 19 nM representing only a 6-fold cell shift (Table 1). Replacement of the P3 cyanophenyl group with an optimized 3-propynylpyridine<sup>20,21</sup> improved the affinity and cell potency, producing an inhibitor 28 with a single-digit nanomolar IC<sub>50</sub> (8.0 nM) in the cell-based assay. Unfortunately, many of these analogues (e.g., compounds 26–28, Table 1) displayed only modest plasma exposures in rat PK studies,<sup>25</sup> possibly due to their susceptibility to P-glycoprotein (P-gp) efflux<sup>26</sup> or high hepatic clearance (e.g., 27, Caco-2 efflux ratio = 17, rat hepatocyte clearance = 46  $\mu\text{L}/\text{min}/10^6$  cells).

To improve the PK profile of this new series, we focused on SAR exploration near the S2' subsite while retaining the previously optimized substituents in the S1 and S3 subsites. In particular, we envisioned that replacements for the amide linkage would be beneficial to the overall properties of the

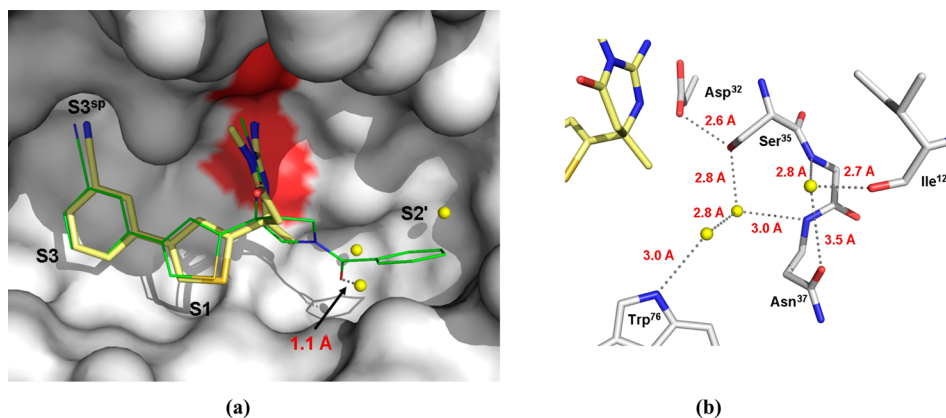
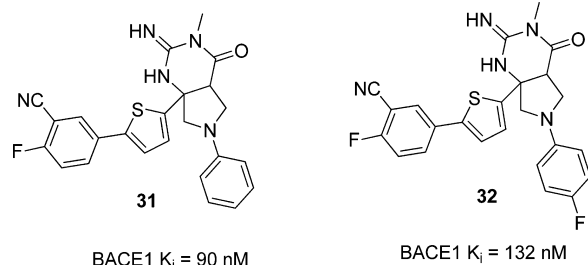


Figure 4. (a) Superimposition of docking conformation of proposed compound 26 (green) with X-ray conformation of 7 (yellow, PDB ID code: 4HAS) showing the pseudoaxial orientation of the biaryl substituent spanning from S1–S3 to S3<sup>sp</sup>. Three conserved water molecules (yellow spheres) are in or near the S2' pocket site when 7 is bound. Docking studies show that one of the water molecules would be ~1.1 Å from the modeling position of the amide oxygen of target 26. (b) Details of the hydrogen bonding network of the three conserved water molecules with the protein backbone of BACE1.

molecule.<sup>27</sup> Docking studies showed that a phenyl group directly linked to the pyrrolidine nitrogen would occupy a pocket that we have termed S2'' that is distinct from the S2' binding pocket occupied by the amides and would also provide opportunities to reach the S2' site with appropriate substitution. In this direction, the first two examples (compounds **31** and **32**, Figure 6) were prepared as racemates



**Figure 6.** BACE1 affinity of racemic **31** and **32**.

using a 2,5-disubstituted thiophene as the S1 substituent and were found to have BACE1 affinities of 90 nM and 124 nM, respectively. Subsequent investigations using both P1 2,5- and 2,4-disubstituted thiophenes showed that the 2,4-substitution pattern provided slightly superior BACE1 inhibition. For example, as shown in Table 2, *N*-fluorophenyl analogue **33** in the 2,4-disubstituted thiophene series was 2.6-fold more potent than **32**. Although compound **33** was 9-fold less potent than benzamide **26**, we were quickly able to restore single-digit nanomolar BACE1 affinity by introduction of an *m*-isopropoxy group on the phenyl in combination with the P3 3-propynylpyridine moiety (cf. **35**). Gratifyingly, compound **35** possessed significantly improved oral rat PK properties (rat  $AUC_{0-6\text{ h}} = 3.7\ \mu\text{M}\cdot\text{h}$ ) compared to its amide counterpart **26**.

On the basis of the observation that inhibitors with lower ClogP generally have lower cell shifts, we next sought to incorporate heteroatoms into the molecule. Strategically, the new *N*-aryl substituent in the S2'' region provided an excellent opportunity for this effort. As shown in the X-ray crystal

structure of compound **31** complexed with BACE1 (Figure 7), the *N*-phenyl group occupies the S2'' site. Interestingly, one of

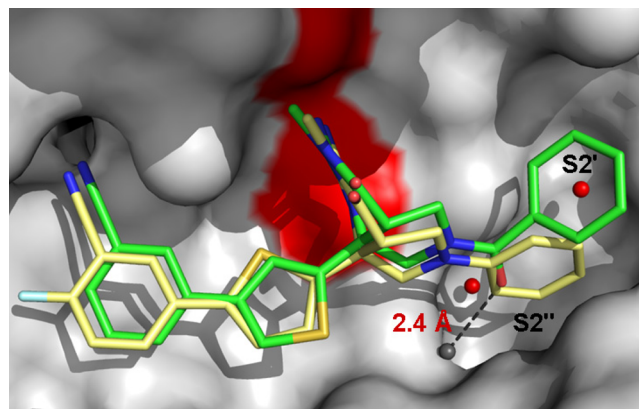


**Figure 7.** Superimposition of X-ray crystal structures of **31** (yellow, PDB ID code: 4H3J) and **26** (green, PDB ID code: 4H1E) complexed with BACE1. The gray ball represents the displaced water molecule, which is 2.4 Å away from the ortho position of the phenyl ring, and its coordinates are taken from the crystal structure of **26** complexed with BACE1. The active site flap residues of BACE1 are omitted for ease of viewing, but despite significant movement or displacement of water molecules in the S2'' region, no significant movement of the flap was observed.

the conserved water molecules positioned between the carbonyl of amide **26** and Trp<sup>76</sup> was displaced in the crystal structure of compound **31**. The proximity of this water molecule to the ortho position of the *N*-phenyl group (2.4 Å) suggested that replacement of the *N*-phenyl with a *N*-pyridin-2-yl would allow for a hydrogen bonding interaction and thus re-establish the original network of water molecules.

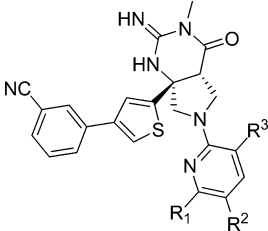
To test this proposal, *N*-pyridyl compound **36** was prepared, and it showed improvements in both BACE1  $K_i$  and cell  $A\beta$   $IC_{50}$  values over *N*-phenyl analogue **33** (Table 3). Both the 3-methoxypyridyl and 3-cyanopyridyl analogues **37** and **38** were well tolerated, and the X-ray crystal structure of compound **37**

**Table 2.** SAR of *N*-Phenyl Derivatives **33**–**35**

cpd	R <sup>1</sup>	R <sup>2</sup>	R <sup>3</sup>	MW (ClogP)	BACE1 $K_i$ (nM) <sup>a</sup>	HEK293 $IC_{50}$ (nM) <sup>a</sup>	LE	CatD/BACE1 <sup>b</sup>	Rat $AUC_{0-6h}$ ( $\mu\text{M}\cdot\text{hr}$ ) <sup>c</sup>
<b>33</b>		F	H	445 (3.9)	26	191	0.32	12	n.d. <sup>d</sup>
<b>34</b>		H	<i>O</i> - <i>i</i> Pr	486 (4.7)	15	308	0.30	17	n.d. <sup>d</sup>
<b>35</b>		H	<i>O</i> - <i>i</i> Pr	499 (4.4)	2	13	0.34	82	3.7

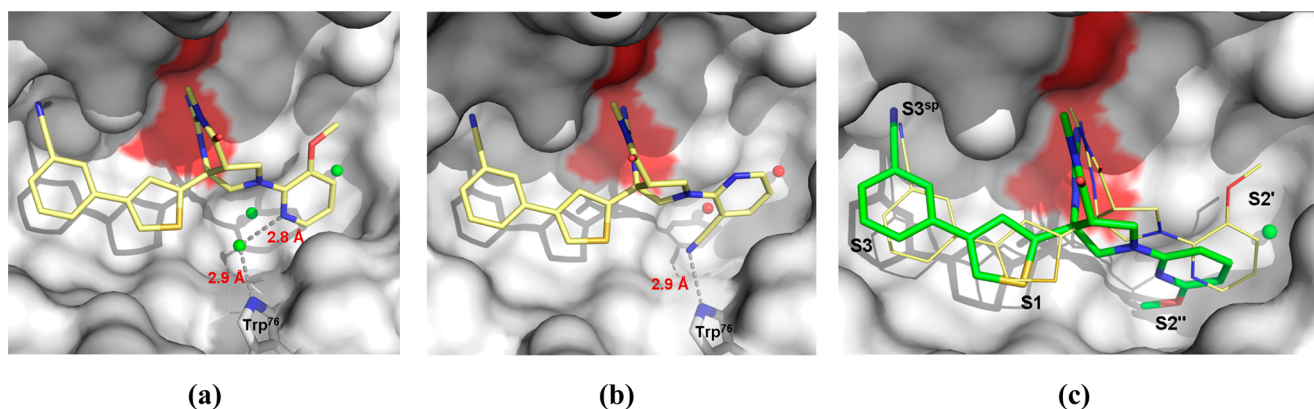
<sup>a</sup>BACE1  $K_i$  and cell  $IC_{50}$  values are the average of a minimum of two independent determinations. <sup>b</sup>Selectivity ratios were derived from cathepsin-D  $K_i$  values (average of a minimum of two independent determinations). <sup>c</sup>Oral dose 10 mg/kg. <sup>d</sup>Not determined.

Table 3. Selected SAR of Pyridine Derivatives 36–41



compd	R <sup>1</sup>	R <sup>2</sup>	R <sup>3</sup>	MW (ClogP)	BACE1 K <sub>i</sub> (nM) <sup>a</sup>	HEK293 IC <sub>50</sub> (nM) <sup>a</sup>	LE	Cath-D/BACE1 <sup>b</sup>
36	H	H	H	428 (2.7)	8	50	0.36	23
37	H	H	OMe	458 (3.1)	3	23	0.35	42
38	H	H	CN	454 (2.3)	6	48	0.34	39
39	H	F	H	446 (2.9)	6	22	0.35	15
40	OMe	H	H	458 (3.5)	1	18	0.37	89
41	CF <sub>3</sub>	H	H	496 (3.7)	64	nd <sup>c</sup>	0.28	nd <sup>c</sup>

<sup>a</sup>BACE1 K<sub>i</sub> and cell IC<sub>50</sub> values are the average of a minimum of two independent determinations. <sup>b</sup>Selectivity ratios were derived from cathepsin-D K<sub>i</sub> values (average of a minimum of two independent determinations). <sup>c</sup>Not determined.



**Figure 8.** (a) Co-crystal structure of 37 (yellow, PDB ID code: 4H3I) in BACE1; the emerging water molecule is 2.8 Å away from the pyridine nitrogen and 2.9 Å away from the NH of the Trp<sup>76</sup>. For clarity, the rest of the H-bonding network depicted in Figure 4b is omitted. (b) X-ray crystal structure of 38 (PDB ID code: 4H3G) complexed with BACE1; the cyano group displaces one of the conserved water molecules and makes direct contact the Trp<sup>76</sup>. (c) X-ray crystal structure of 40 (green, PDB ID code: 4H3F) complexed with BACE1; the methoxy group occupies the S2'' subsite, displacing two of the conserved water molecules. Superimposition with X-ray conformation of 37 (yellow) shows that 40 moves almost 1.0 Å toward the S2'' binding pocket. As in Figure 7, the flap residues are omitted from these figures, but again no significant movement of the flap of was observed despite changes in the binding mode and water molecule organization.

(Figure 8a) demonstrated reincorporation of the water molecule connecting the pyridine nitrogen and the NH of Trp<sup>76</sup>, recapitulating the network previously observed with compound 26. In contrast, the 3-cyanopyridyl analogue 38 bound in the opposite orientation with the nitrile projected deep into the S2'' binding pocket. This conformation again displaced a conserved water molecule from the hydrogen-bond network to establish a direct hydrogen bond between the nitrile and the NH of Trp<sup>76</sup> (Figure 8b).

Turning to the 6-position of pyridyl, while introduction of a lipophilic group like trifluoromethyl (e.g., 41) was not tolerated, incorporation of a methoxy group resulted in an 8-fold boost in affinity, with compound 40 having a BACE1 K<sub>i</sub> of 1 nM. The X-ray crystal structure of 40 complexed with BACE1 showed that the inhibitor shifted almost 1.0 Å toward the nonprime side of the enzyme to bury the methoxy pyridine into the S2'' subpocket and displace a second conserved water molecule from this region (Figure 8c). The in-plane *anti*-oriented methoxy group, a result of lone pair/lone pair repulsion between the pyridine nitrogen and the ether oxygen,<sup>28</sup> positions the methoxy group in the deepest part of

S2''. Overall, replacement of the *N*-(4-fluoro)phenyl group with an appropriately substituted pyridyl resulted in a 26-fold improvement in BACE1 affinity (c.f., 33 vs 40).

While beneficial for affinity and cellular potency, introduction of the S2'' pyridyl group consistently resulted in inhibition of CYP<sub>450</sub> enzymes. For example, compound 39 inhibited 2D6 and 3A4 with IC<sub>50</sub> values of 6 μM each. Thus, we next focused on less basic heterocyclic replacements of the S2'' pyridine ring in an attempt to improve the CYP inhibition profile. The X-ray structures of analogues 38 and 40 complexed with BACE1 (Figure 8b,c) demonstrated that compounds with the *N*-pyridyl nitrogen oriented either toward S2' (e.g., 38) or toward S2'' (e.g., 40) were essentially equipotent, suggesting that an *N*-pyrimidyl group should itself be well tolerated. In fact, pyrimidine 42 was equipotent with the analogous pyridine 36 against BACE1 with no CYP<sub>450</sub> inhibition. In a rat oral PK screen with 10 mg/kg of compound 42, a C<sub>max</sub> of 1 μM was observed at 1 h with plasma levels decreasing to 0.06 μM at 6 h and a 6 h brain-to-plasma ratio of 1. On the basis of its promising profile, albeit with low plasma and brain concentrations at the 6 h time point, compound 42 was

Table 4. Selected SAR of Pyrimidine Derivatives 42–45

compd	R <sup>1</sup>	MW (ClogP)	BACE1 K <sub>i</sub> (nM) <sup>a</sup>	HEK293 IC <sub>50</sub> (nM) <sup>a</sup>	LE	Cath-D/BACE1 <sup>b</sup>	rat AUC <sub>0–6h</sub> (μM·h) <sup>c</sup>	brain 6 h (μM)	brain/plasma	rat PPB <sup>d</sup> (% unbound)
42	H	429 (1.9)	11	31	0.35	28	2.0	0.058	1.0	2.2
43	F	447 (2.1)	4	16	0.36	94	31	0.463	0.1	2.4
44	Cl	464 (2.6)	7	51	0.35	81	90	0.965	0.1	0.4
45	Me	443 (2.4)	9	29	0.34	67	111	0.232	<0.1	nd <sup>e</sup>

<sup>a</sup>BACE1 K<sub>i</sub> and cell IC<sub>50</sub> values are the average of a minimum of two independent determinations. <sup>b</sup>Selectivity ratios were derived from cathepsin-D K<sub>i</sub> values (average of a minimum of two independent determinations). <sup>c</sup>Oral dose 10 mg/kg. <sup>d</sup>Plasma protein binding. <sup>e</sup>Not determined.

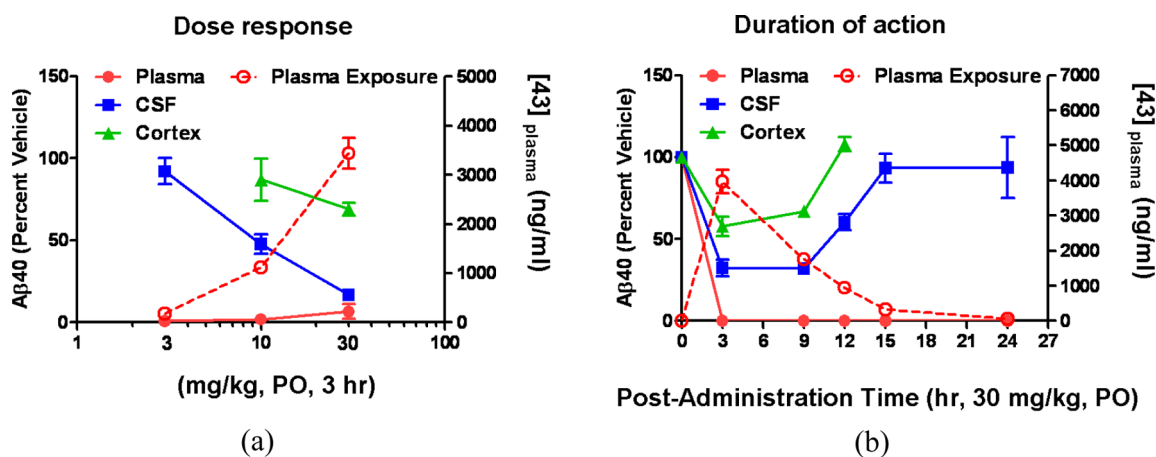


**Figure 9.** (a) Dose-dependent inhibition of Aβ<sub>40</sub> production in the plasma, CSF, and cortex compartments of rats by compound 43 measured at 3 h period after oral administration. (b) Post dose (30 mg/kg) measurements in plasma, CSF, and cortex revealed that the level of Aβ<sub>40</sub> remained inhibited in cortex and CSF until 9 h after dosing and in plasma until 24 h after dosing.

screened in vivo for central efficacy in rats. However, compound 42 did not produce a significant reduction of CSF Aβ<sub>40</sub> in the CSF following a single oral 10 mg/kg dose. This lack of efficacy is likely due to a very low level of compound in the brain considering that, from the rat PK data in Table 4, there is a free concentration of only approximately 1 nM in the brain at 6 h.<sup>29</sup> This result suggested that further improvement in potency and PK to increase *t*<sub>1/2</sub> and brain exposure was necessary.

Through introduction of a substituent at the 5-position of the pyrimidine, we identified three compounds (43–45), bearing 5-fluoro, -chloro, and -methyl groups, respectively, with good affinity as well as improved oral exposure and 6 h absolute brain levels in rat. Compounds 43 and 44 were selected over 45 for in vivo screening due to their higher 6 hour brain levels (Table 4). Of these two compounds, only fluoropyrimidine 43 showed robust lowering of CSF Aβ<sub>40</sub> following a 10 mg/kg oral dose (52% Aβ<sub>40</sub> lowering for 43 versus 15% for 44), even though both compounds had similar total brain levels. To explain this discrepancy, we speculate that again free fraction plays an important role: chloropyrimidine 44 has a significantly lower unbound fraction (0.4%) than fluoropyrimidine 43 (2.4%). When these free fractions are applied to the total brain levels from the rat PK data in Table 4,<sup>29</sup> the free drug level for

compound 44 is only 4 nM versus 11 nM for compound 43. The latter free concentration is close to the cellular IC<sub>50</sub> of the compound. This delicate balance underscores the critical importance of physicochemical properties, particularly the interplay of lipophilicity and free fraction, on PK and thus CNS efficacy.

Upon further in vivo evaluation, compound 43 was found to dose-dependently reduce Aβ<sub>40</sub> in plasma, CSF, and cortex of rats. Complete inhibition of Aβ<sub>40</sub> in plasma was observed with oral doses as low as 3 mg/kg (Figure 9a). In the central compartments, administration of compound 43 (10 mg/kg PO) produced 50% reduction of CSF Aβ<sub>40</sub> at 3 h postdose, while 30 mg/kg produced 73% and 42% reduction of CSF and cortical Aβ<sub>40</sub>, respectively (Figure 9a). In a time course study (Figure 9b) using a single oral 30 mg/kg dose of compound 43, the levels of Aβ<sub>40</sub> in the CSF and cortex remained inhibited for 9 h before returning to baseline at 15 and 12 h, respectively. Maximal inhibition of Aβ<sub>40</sub> in both CNS compartments occurred at *t*<sub>max</sub> for plasma concentration (3 h post dose) and continued for approximately one-half-life of exposure (i.e., out to 9 h post dose).

In terms of its broader profile, compound 43 is nearly 100-fold selective for BACE1 over cathepsin-D, making it the most selective of the analogues discussed herein from this new series



Table 5. Rat Pharmacokinetic Properties of 43

AUC <sub>0–24 h</sub> <sup>a</sup>	PO C <sub>max</sub> μM	B/P (6 h)	P <sub>app</sub> (nm/s)	efflux ratio	P450 enzyme inhibition μM-co, μM-po			<i>h</i> -ERG patch clamp
					3A4	2D6	2C9	
31	6.1	0.1	151	1.9	>30, 1.9	30, 19.7	22.4, 30	70% @ 1 μM
hepatocyte Cl <sub>int</sub> μL·min <sup>-1</sup> ·10 <sup>-6</sup> cells								
rat		human		cyno monkey		F%	rat fu <sub>pl</sub> <sup>b</sup>	<i>h</i> -PXR (over rifampicin)
13.5	2.0		5.7	97		0.024		0.2X @ 10 μM

<sup>a</sup>Oral dose 10 mg/kg. <sup>b</sup>Fraction unbound in plasma.

(Tables 1–4). While this compound does not cause induction of human *h*-PXR, it is a time-dependent inhibitor of CYP<sub>450</sub> 3A4 and showed significant inhibition of the *h*-ERG channel in a patch clamp assay (Table 5). Compound 43 showed a significantly reduced efflux ratio in Caco-2 cells (Table 5) compared to amide-containing analogue 27 (1.9 vs 17), although even with this lower ratio the compound may be a substrate for P-gp given its low brain-to-plasma ratio in rats. This compound also showed low to moderate in vitro hepatocyte clearance across species. Overall, while still requiring further optimization to address these ancillary issues, compound 43 provided a key proof-of-concept for this new series, showing that this significantly modified core structure could confer robust central efficacy.

## SUMMARY AND CONCLUSION

As part of efforts to further optimize a lead iminopyrimidinone BACE1 inhibitor 7, a structure-based design approach enabled discovery of a structurally distinct fused pyrrolidine series. Although the conformational constraint of this novel bicyclic core was designed both to favor the bioactive conformer and to explore SAR in the S2' region, we found that gains in potency did not have accompanying gains in ligand efficiency. This disconnect may be due to the only modest bias for the pseudoaxial conformation conferred by the fused five-membered ring, which was predicted to favor the bioactive conformation by roughly 1 kcal/mol. On the other hand, the fused ring provided an ideal platform to reach into and study the SAR of both the S2' and the S2'' binding pockets, ultimately providing a number of potent analogues. Initial *N*-carboxamide compounds in this series (e.g., compound 26) showed good binding affinity but suffered from poor pharmacokinetic properties. Moving to *N*-aryl analogues ultimately provided compounds that had excellent potency and demonstrated significantly improved PK, validating an emphasis on optimization of drug-like properties during SAR development. A close collaboration with structural chemistry and chemical modeling and informatics facilitated our understanding of the importance of a network of hydrogen bound waters in the S2'' subpocket and drove additional targeted modifications. Ultimately, these investigations, in conjunction with the efforts from in vitro and in vivo pharmacology, led to identification of compound 43, an orally active brain penetrant inhibitor that potently reduced central Aβ<sub>40</sub> in rats. Further modifications to this series aimed at improving the pharmacological and off-target profile will be the subject of a future communication.

## EXPERIMENTAL SECTION

Details of the protocols for X-ray crystallography, aspartyl protease K<sub>p</sub> and cell Aβ<sub>40</sub> IC<sub>50</sub> assays and in vivo rat CSF studies can be found in ref 21.

**Relative Energy Calculations.** Conformational searches for compounds 7 and 7a were carried out using the MacroModel method in the Schrödinger modeling package.<sup>30</sup> Each compound was subjected to 3000 steps of mixed torsional/low-mode sampling using MMFFs force field to find the low energy conformations within 10 kcal/mol above the global energy minimum. Quantum mechanics (QM) energy optimizations were then carried out on these low energy conformations. QM method Jaguar in Schrodinger package was used for the QM calculations. The B3LYP hybrid density functional and the 6-31G\*\* basis set were used in geometry optimizations. The lowest QM energy of the pseudoaxial conformation and that of the pseudoequatorial conformation for each compound were used to calculate the energy differences.

**Synthesis.** Unless otherwise mentioned, all the reagents and solvents were obtained from commercial sources and used without further purification. Air sensitive chemistries were performed under an atmosphere of nitrogen or argon. Purification of the final compounds to >95% purity were carried out either using prepacked silica gel cartridge (Analogix or Biotage or ISCO) or reverse phase C18 column (mobile phase, A = 0.05% TFA in water and B = 0.05% TFA in acetonitrile, gradient = 10–95% B over 10 min). All NMR data were collected using 400 MHz NMR spectrometry, and the chemical shifts are listed as ppm relative to tetramethylsilane. Microwave assisted reactions were performed in a Smith synthesizer from Personal Chemistry. The purity of final compounds was analyzed on two independent reverse phase HPLC systems using different gradients. LC-electrospray-mass spectrometry with a C-18 column using a gradient of 5–95% MeCN in water as the mobile phase was used to determine the molecular mass and retention time. The purity of the samples was assessed using a mass detector and a UV detector at 254 nm. An additional analytical reverse phase HPLC system was used to assess the purity of final compounds using a UV detector monitored at both 220 and 254 nm and an ELSD detector.

**(4aR,7aR)-2-(Trimethylsilyl)ethyl 7a-(4-Bromothiophen-2-yl)-2-((*tert*-butoxycarbonyl)imino)-3-methyl-4-oxohexahydro-1*H*-pyrrolo[3,4-*d*]pyrimidine-6(2*H*)-carboxylate (22).** To a solution of aldehyde 8 (20 g, 105 mmol) in methanol (100 mL) was added NaBH<sub>4</sub> (4.0 g, 108 mmol) portionwise at 0 °C. The resulting solution was stirred at 0 °C for 2 h. Water (100 mL) was added slowly, and the resulting mixture was stirred at 0 °C until gas evolution had ceased. The ice bath was removed, and the solution was stirred at room temperature for 30 min before evaporation to dryness. The resulting slurry was extracted with ethyl acetate (3 × 100 mL). The organic layers were combined and washed with brine, dried with MgSO<sub>4</sub>, and evaporated to provide the corresponding alcohol. The crude alcohol was >95% pure by <sup>1</sup>H NMR and used directly in next step. <sup>1</sup>H NMR (400 MHz, CDCl<sub>3</sub>) δ 7.17 (s, 1H), 6.93 (s, 1H), 4.80 (d, *J* = 6.0 Hz, 2H), 1.84 (t, *J* = 6.0 Hz, 1H). To a solution of this alcohol (20 g 103 mmol) in CH<sub>2</sub>Cl<sub>2</sub> (10 mL) was added SOCl<sub>2</sub> (14.5 g, 124 mmol) slowly at 0 °C. The resulting reaction mixture was stirred at 0 °C until the gas evolution had ceased. The ice bath was removed, and the reaction mixture was slowly warmed to room temperature and stirred at room temperature for 12 h. The reaction mixture was evaporated to dryness, and the resulting slurry was diluted with ethyl acetate and washed with brine. The organic layer was dried with MgSO<sub>4</sub> and evaporated to yield the chloride 9 (20 g, 98%). The crude chloride was >95% pure by <sup>1</sup>H NMR and directly used in the next step

without further purification.  $^1\text{H}$  NMR of **9** (400 MHz,  $\text{CDCl}_3$ )  $\delta$  7.15–7.30 (m, 2H), 4.73 (s, 2H).

To a solution of chloride **9** (4.4 g, 21 mmol) in 50 mL of acetonitrile was added oven-dried KCN (5 g, 76 mmol) portionwise. The resulting mixture was stirred at room temperature for 1 h and then heated under reflux for 20 h until the reaction was completed. The reaction mixture was diluted with ethyl acetate (100 mL) and filtered, the solid was washed with ethyl acetate (3  $\times$  50 mL), and the combined filtrate was evaporated. The residue was purified by silica gel chromatography using 10% ethyl acetate/hexanes to give nitrile **10** (3.1 g, 75%).  $^1\text{H}$  NMR of **10** (400 MHz,  $\text{CDCl}_3$ )  $\delta$  7.18 (s, 1H), 7.0 (s, 1H), 3.89 (s, 2H).

Compound **11** was prepared following a literature procedure.<sup>22</sup> To a solution of **10** (4 g, 20 mmol) and glyoxaldehyde (4.2 g, 30 mmol, 50% aq solution) in MeOH (50 mL) was added  $\text{K}_2\text{CO}_3$  (6.9 g, 50 mmol), and the reaction mixture was stirred at room temperature for 4 h. The reaction mixture was filtered, and the solid was washed with ether. The solid was suspended in cold water and stirred vigorously for 1 h. The solid was filtered and dried to give crude product **11** (5.12 g, 100%). A small quantity of **11** was dissolved in water, neutralized with 1N HCl, and extracted with EtOAc. The organic solution was evaporated to give the corresponding free acid of **11**.  $^1\text{H}$  NMR (400 MHz,  $\text{CDCl}_3$ ) of **11** as a free acid:  $\delta$  7.69 (s, 1H), 7.56 (s, 1H), 6.96 (s, 1H).

To a solution of **11** (50 g, 193 mmol) in formic acid (mL) was added concd sulfuric acid (40 mL). The resulting solution was heated under reflux for 2 h. The reaction was cooled to room temperature and poured into ice water, and the solid was filtered to give the anhydride of product **12**. This anhydride was dissolved in the mixture of  $\text{CH}_3\text{CN}-\text{H}_2\text{O}$  (9:1) was heated at 40  $^\circ\text{C}$  for 12 h. The reaction solution was concentrated and the residue dried to give compound **12** (56 g, 100%).  $^1\text{H}$  NMR of **12** (400 MHz,  $\text{CDCl}_3$ )  $\delta$  7.66 (s, 1H), 7.40 (s, 1H), 6.42 (s, 1H).

To a solution of **12** (5 g, 18.17 mmol) in anhydrous THF (72 mL) was added *N*-benzyl-1-methoxy-*N*-((trimethylsilyl)methyl)-methanamine (8.61 g, 37 mmol) at 0  $^\circ\text{C}$ , and the resulting mixture was stirred at 0  $^\circ\text{C}$  for 90 min. It was then quenched with 1N HCl (10 mL) and extracted with ethyl acetate (3  $\times$  50 mL). The organic layers were combined, dried with anhydrous  $\text{Na}_2\text{SO}_4$ , and concentrated to provide **14** (6 g, 82%), which was used in the next step without further purification.  $^1\text{H}$  NMR of **14** (400 MHz,  $\text{CDCl}_3$ )  $\delta$  7.45–7.60 (m, 7H), 4.49 (m, 2H), 4.30 (d,  $J$  = 12.0 Hz, 1H), 3.8–4.0 (m, 4H).

To an oven-dried flask containing **14** (6 g, 14.6 mmol) was added acetic anhydride (100 mL) at room temperature. The resulting solution was heated for 30 min at 90  $^\circ\text{C}$  and then allowed to cool to room temperature. The reaction mixture was evaporated to dryness to provide crude anhydride **15**, which was poured into a flask containing methanol (500 mL) at 0  $^\circ\text{C}$ . The resulting solution was slowly warmed to room temperature and evaporated to dryness. The crude product was dissolved in  $\text{CH}_2\text{Cl}_2$  (200 mL) and washed with 1H HCl (50 mL), followed by with brine, and then dried with  $\text{Na}_2\text{SO}_4$  and concentrated to provide **16** (6 g, 96%), which was used in the next step without purification.  $^1\text{H}$  NMR of **16** (400 MHz,  $\text{CDCl}_3$ )  $\delta$  7.10–7.60 (m, 7H), 4.3 (m, 2H), 4.12 (d,  $J$  = 12.0 Hz, 1H), 3.7–3.9 (m, 4H), 3.6 (s, 3H).

To an oven-dried flask containing **16** (4.67 g, 11 mmol) in toluene (10 mL) was added DPPA (3 mL, 14.18 mmol), followed by triethyl amine (2.16 mL, 24.2 mmol) at 0  $^\circ\text{C}$ . The resulting mixture was slowly warmed to room temperature and stirred for 12 h. To the reaction mixture was added trimethylsilylethanol (4 mL, 44 mmol), and the reaction mixture was heated under reflux for 1 h, then it was cooled to room temperature, diluted with ethyl acetate (150 mL), and washed with brine and water. The organic layer was dried with  $\text{Na}_2\text{SO}_4$ , filtered, and concentrated in vacuo. The crude product was purified by silica gel chromatography using 30% ethyl acetate in hexanes to provide **17** (1.5 g, 40%).  $^1\text{H}$  NMR of **17** (400 MHz,  $\text{CDCl}_3$ )  $\delta$  7.20–7.40 (m, 5H), 7.07 (d,  $J$  = 1.5 Hz, 1H), 6.94 (d,  $J$  = 1.5 Hz, 1H), 4.11 (m, 2H), 3.79 (d,  $J$  = 11 Hz, 1H), 3.70 (s, 3H), 3.69 (d,  $J$  = 11 Hz, 1H), 3.54 (d,  $J$  = 10 Hz, 1H), 3.32 (t,  $J$  = 8 Hz, 1H), 3.21 (d,  $J$  = 10 Hz, 1H), 3.16 (t,  $J$  = 8 Hz, 1H), 2.88 (t,  $J$  = 8 Hz, 1H), 0.97 (m, 2H), 0.03 (s, 9H).

To a solution of **17** (35.2 g, 65 mmol) in dioxane (200 mL) was added 4N HCl (20 mL) in dioxane at 0  $^\circ\text{C}$ , and the resulting solution was allowed to warm to room temperature over 14 h. Ether (400 mL) was added to form a white precipitate. This precipitate was collected, washed with ether (200 mL), and dried in vacuo for 12 h to give **18** (28 g, 100%) as a HCl salt, which was used without further purification.  $^1\text{H}$  NMR of **18** (400 MHz,  $\text{CDCl}_3$ ) of the product amine HCl salt:  $\delta$  7.20–7.40 (m, 5H), 7.17 (d,  $J$  = 1.5 Hz, 1H), 6.86 (d,  $J$  = 6.86 Hz, 1H), (3.65 (m, 1H), 3.45–3.31 (m, 6H), 3.29 (s, 3H).

To a solution of **18** (32 g, 76 mmol) in DMF (300 mL) was added DIEA (66 mL, 380 mmol), *t*-butyl *N*-[(methylamino)thioxomethyl]-carbamate (14.4 g, 76 mmol) and followed by EDCI-HCl (14.5 g, 76 mmol), and the resulting mixture was stirred at room temperature for 48 h. It was then diluted with ethyl acetate (150 mL), washed with brine, and water. The organic layer was dried with  $\text{Na}_2\text{SO}_4$  and concentrated. The crude product was purified by silica gel chromatography using 0–100% ethyl acetate in hexanes to provide **19** (23 g, 60%).  $^1\text{H}$  NMR of **19** (400 MHz,  $\text{CDCl}_3$ )  $\delta$  7.25–7.34 (m, 5 H), 7.15 (d,  $J$  = 1.5 Hz, 1H), 6.91 (d,  $J$  = 1.5 Hz, 1H), 3.75 (m, 2H), 3.42 (m, 1H), 3.34 (m, 1H), 3.31 (s, 3H), 3.22 (d,  $J$  = 10 Hz, 1H), 3.09 (d,  $J$  = 10 Hz, 1H), 3.02 (m, 1H), 1.54 (s, 9H).

To a solution of **19** (1.0 g, 1.9 mmol) in DCM (10 mL) was added potassium carbonate (0.3 g, 2.0 mmol) followed by 1-chloroethylchloroformate (0.269 g, 1.9 mmol) at –15  $^\circ\text{C}$ , and the resulting solution was slowly warmed to room temperature and stirred for 90 min. The reaction mixture was filtered, and the filtrate was evaporated. The residue was dissolved in methanol (10 mL) and stirred overnight. After removal of methanol in vacuo, the residue was purified by silica gel chromatography using 10% methanol in dichloromethane to give **20** (0.570 g, 70% yield).  $^1\text{H}$  NMR of **20** (400 MHz,  $\text{CDCl}_3$ )  $\delta$  10.30 (br s, 1H), 7.17 (d,  $J$  = 1.5 Hz, 1H), 6.86 (d,  $J$  = 1.5 Hz, 1H), 3.68 (m, 1H), 3.42 (d,  $J$  = 12 Hz, 1H), 3.31–3.40 (m, 3H), 3.29 (s, 3H), 1.52 (s, 9H).

To a solution of **20** (13 g, 30 mmol) in DCM (100 mL) was added Teoc-OSu (7.7 g, 30 mmol) followed by DIEA (5.2 mL, 30 mmol) at 0  $^\circ\text{C}$ . The reaction was stirred for 6 h. The reaction mixture was diluted with ethyl acetate and washed with water and brine. The organic layer was dried and evaporated, and the residue was purified by silica gel chromatography using 20% ethyl acetate in hexanes to give **21** (13.7 g, 80%).  $^1\text{H}$  NMR (400 MHz,  $\text{CDCl}_3$ )  $\delta$  10.40 (br m, 1H), 7.22 (br s, 1H), 6.90 (br s, 1H), 4.20 (m, 2H), 3.68–4.06 (m, 4H), 3.47 (m, 1H), 3.30 (s, 3H), 1.29 (s, 9H), 1.01 (m, 2H), 0.03 (s, 9H). *m/z*: 595.22. **21** was resolved using a semipreparative ChiralPak AS column eluted with 50% isopropyl alcohol in hexane (50 mL/min). Enantiomer A, **22**:  $t_R$  = 19.3 min,  $[\alpha]_D^{25} = -94^\circ$  (MeOH,  $C$  = 1, 23  $^\circ\text{C}$ ). Enantiomer B, ent-**22**:  $t_R$  = 39.5 min,  $[\alpha]_D^{25} = +105^\circ$  (MeOH,  $C$  = 1, 23  $^\circ\text{C}$ ).

**General Procedure A for Synthesis of Pyrrolidine 23–25 and 30.** To a solution of bromide **22** (1.74 mmol) and boronic acid (2.61 mmol) in *t*-BuOH (7 mL) was added dichloro[1,1'-bis-(diphenylphosphino)-ferrocene]palladium(II) dichloromethane (0.190 g, 0.261 mmol) followed by aqueous 1N  $\text{K}_2\text{CO}_3$  (2.61 mL, 2.61 mmol). The resulting mixture was heated at 60  $^\circ\text{C}$  for 1 h before it was cooled, diluted with ethyl acetate, and washed with water. The organic layer was dried and concentrated, and the residue was purified by silica gel chromatography using 0–100% ethyl acetate in hexanes to provide the product. To this product (0.963 g, 1.56 mmol) was added 1 M TBAF (5 mL, 5 mmol) in THF at 0  $^\circ\text{C}$ , and the solution was stirred at room temperature for 4 h. The reaction mixture was poured into a saturated solution of  $\text{NaHCO}_3$  and extracted with ethyl acetate. The organic layer was concentrated, and residue was purified by silica gel chromatography using 100% ethyl acetate to give pyrrolidines **23–25**.

**General Procedure B for Synthesis of Compounds 26–28.** To a solution of pyrrolidine (1 mmol) in dichloromethane (5 mL) were added HOBt (1 mmol), benzoic acid (1 mmol), and DIEA (1 mmol) followed by EDCI-HCl (1 mmol) and the solution was stirred for 3 h. The reaction mixture was diluted with water and extracted with EtOAc (3  $\times$  50 mL). The organic layer was dried and concentrated, and the residue was purified by silica gel chromatography using 0–

100% ethyl acetate in hexanes to give the product, which was subsequently deprotected with 20% TFA/DCM (2 mL). The deprotected compounds were purified by reverse phase C18 column using 0–90% water (0.05% TFA) in acetonitrile (0.05% TFA).

#### General Procedure C for Synthesis of Compounds 33–35.

To a solution of pyrrolidine (1 mmol) in DCM (5 mL) was added boronic acid (1 mmol), Cu(OAc)<sub>2</sub> (1 mmol), triethylamine (2 mmol), and preactivated 4 Å molecular sieves (5 μm, 200 mg). The resulting mixture was stirred for 48 h, whereupon the solid was filtered and the organic solution was concentrated. The residue was purified by silica gel chromatography using 0–100% ethyl acetate in hexanes to give the product which was deprotected with 20% TFA/DCM (2 mL). The deprotected compounds were purified by reverse phase C18 column using 0–90% water (0.05% TFA) in acetonitrile (0.05% TFA).

**General Procedure D for the Synthesis of Compounds 31–32 and 36–45.** To a solution of pyrrolidine (1 mmol) and corresponding hetero halide (1 mmol) in toluene (2 mL) was added tris(dibenzylidene-acetone)dipalladium(0) (0.07 mmol), BINAP (0.14 mmol), and NaOt-Bu (1.2 mmol). The resulting solution was degassed and heated at 70 °C for 3 h and then cooled to room temperature and filtered through a pad of Celite, and the crude material was purified by silica gel chromatography using 0–100% EtOAc/hexanes to give the product which was treated with 20% TFA/DCM (2 mL). The deprotected compounds were purified by reverse phase C18 column using 0–90% acetonitrile (0.05% TFA) in water (0.05% TFA).

**tert-Butyl ((4aR,7aR)-7a-(4-(3-Cyanophenyl)thiophen-2-yl)-3-methyl-4-oxohexahydro-1H-pyrrolo[3,4-d]pyrimidin-2(3H)-ylidene)carbamate (23).** Compound 23 was prepared from 22 in two steps following the general procedure A. <sup>1</sup>H NMR (400 MHz, CDCl<sub>3</sub>) δ 10.54 (br s, 1H), 7.78 (m, 1H), 7.73–7.71 (m, 1H), 7.59–7.57 (m, 1H), 7.49 (t, J = 8.0 Hz, 1H), 7.43 (m, 1H), 7.18 (m, 1H), 3.73 (m, 1H), 3.49 (m, 2H), 3.36 (m, 2H), 3.32 (s, 3H), 1.54 (s, 9H). *m/z*: 452.3.

**tert-Butyl ((4aR,7aR)-7a-(4-(3-Cyano-4-fluorophenyl)thiophen-2-yl)-3-methyl-4-oxohexahydro-1H-pyrrolo[3,4-d]pyrimidin-2(3H)-ylidene)carbamate (24).** Compound 24 was prepared following the general procedure A from 22 in two steps. <sup>1</sup>H NMR (400 MHz, CDCl<sub>3</sub>) δ 10.4 (br s, 1H), 7.72 (m, 2H), 7.34 (br s, 1H), 7.25 (m, 2H), 7.13 (m, 1H), 3.72 (m, 1H), 3.46 (m, 7H), 1.53 (s, 9H). *m/z*: 470.2.

**tert-Butyl ((4aR,7aR)-3-Methyl-4-oxo-7a-(4-(5-(prop-1-yn-1-yl)pyridin-3-yl)thiophen-2-yl)hexahydro-1H-pyrrolo[3,4-d]pyrimidin-2(3H)-ylidene)carbamate (25).** Compound 25 was prepared following the general procedure A in two steps from bromide 22. <sup>1</sup>H NMR (400 MHz, CDCl<sub>3</sub>) δ 10.36 (s, 1H), 8.65 (s, 1H), 8.53 (s, 1H), 7.77 (s, 1H), 7.43 (br s, 1H), 7.18 (m, 1H), 3.73 (m, 1H), 3.49 (m, 2H), 3.40 (m, 2H), 3.32 (s, 3H), 2.09 (s, 3H), 1.54 (s, 9H).

**3-(5-((4aR,7aR)-6-Benzoyl-2-imino-3-methyl-4-oxooctahydro-1H-pyrrolo[3,4-d]pyrimidin-7a-yl)thiophen-3-yl)benzotrile (26).** Compound 26 was prepared in two steps from 23 following the general procedure B. <sup>1</sup>H NMR (400 MHz, CD<sub>3</sub>OD) δ 7.94 (m, 2H), 7.57 (m, 9H), 4.47 (m, 0.4H from one rotamer), 4.11 (m, 4.6H), 3.3 (m, 3H). *m/z*: 456.3.

**2-Fluoro-5-(5-((4aR,7aR)-6-(3-fluorobenzoyl)-2-imino-3-methyl-4-oxooctahydro-1H-pyrrolo[3,4-d]pyrimidin-7a-yl)thiophen-3-yl)benzotrile (27).** Compound 27 was prepared from 24 in two steps following the general procedure B. <sup>1</sup>H NMR (400 MHz, CD<sub>3</sub>OD) δ 7.97 (m, 2H), 7.63 (m, 1H), 7.45 (m, 6H), 4.43–3.84 (m, 5H), 3.24 (m, 3H). *m/z*: 492.3.

**(7aR)-6-(3-Fluorobenzoyl)-2-imino-3-methyl-7a-(4-(5-(prop-1-yn-1-yl)pyridin-3-yl)thiophen-2-yl)hexahydro-1H-pyrrolo[3,4-d]pyrimidin-4(4aH)-one (28).** Compound 28 was prepared from 25 in two steps following the general procedure B. <sup>1</sup>H NMR (400 MHz, CD<sub>3</sub>OD) δ 8.83 (br s, 1H), 8.79 (br s, 1H), 8.25 (br s, 0.5H), 8.20 (br s, 0.5H), 7.88 (br s, 0.5H), 7.84 (br s, 0.5H), 7.55–7.25 (m, 5H), 4.50–4.05 (m, 5H), 3.30 (m, 3H), 2.16 (m, 3H). *m/z*: 488.3.

**(4aR,7aR)-2-(Trimethylsilyl)ethyl 7a-(5-Bromothiophen-2-yl)-2-((tert-butoxycarbonyl)imino)-3-methyl-4-oxohexahydro-1H-pyrrolo[3,4-d]pyrimidine-6(2H)-carboxylate (29).** To a sol-

ution of 22 (1.8 g, 3.14 mmol) in methanol (15 mL) was added 10% Pd/C (200 mg), and the resulting solution was stirred for 90 min under an atmosphere of hydrogen. Upon completion of the reaction the reaction mixture was basified using Et<sub>3</sub>N, and then it was filtered and concentrated. The residue was purified by silica gel chromatography using 0–100% ethyl acetate in hexanes to provide the debrominated product (1.3 g, 69%). <sup>1</sup>H NMR (400 MHz, CDCl<sub>3</sub>) δ 10.40 (m, 1H), 7.31 (m, 1H), 6.97–6.99 (m, 2H), 4.20 (m, 2H), 3.68–4.06 (m, 4H), 3.50 (m, 1H), 3.30 (s, 3H), 1.53 (s, 9H), 1.01 (m, 2H), 0.03 (s, 9H). To a solution of the above debrominated product (0.3 g, 2 mmol) in DMF (6 mL) was added NBS (0.42 g, 2.4 mmol), and the reaction was stirred for 12 h. The reaction mixture was diluted with water and extracted with ethyl acetate. The organic layer was dried and concentrated. The residue was purified by silica gel chromatography using 0–100% ethyl acetate in hexanes to provide 29 (0.916 g, 80%). <sup>1</sup>H NMR (400 MHz, CDCl<sub>3</sub>) δ 10.39 (m, 1H), 6.94 (d, J = 4 Hz, 1H), 6.76 (m, 1H), 4.20 (m, 2H), 3.68–4.04 (m, 4H), 3.43 (m, 1H), 3.29 (s, 3H), 1.53 (s, 9H), 1.01 (m, 2H), 0.03 (s, 9H).

**2-Fluoro-5-(5-((4aR,7aR)-2-imino-3-methyl-4-oxo-6-phenyloctahydro-1H-pyrrolo[3,4-d]pyrimidin-7a-yl)thiophen-2-yl)benzotrile (31).** Compound 31 was prepared from 29 in four steps following the general procedure A and followed by general procedure D. <sup>1</sup>H NMR (400 MHz, CD<sub>3</sub>OD) δ 8.03 (dd, J = 2.6, 5.9 Hz, 1 H), 7.95 (ddd, J = 2.4, 5.0, 8.7 Hz, 1 H), 7.44–7.38 (m, 2 H), 7.26–7.19 (m, 3 H), 6.74 (t, J = 7.3 Hz, 1 H), 6.65 (d, J = 8.1 Hz, 2 H), 4.11–4.02 (m, 2 H), 3.95 (d, J = 10.6 Hz, 1 H), 3.89 (m, 2 H), 3.35 (s, 3 H). *m/z*: 446.2.

**2-Fluoro-5-(5-((4aR,7aR)-6-(4-fluorophenyl)-2-imino-3-methyl-4-oxooctahydro-1H-pyrrolo[3,4-d]pyrimidin-7a-yl)thiophen-2-yl)benzotrile (32).** Compound 32 was prepared from 29 in four steps following the general procedure A and followed by general procedure D. <sup>1</sup>H NMR (400 MHz, CD<sub>3</sub>OD) δ 8.03 (dd, J = 2.2, 5.9 Hz, 1 H), 7.95 (ddd, J = 2.2, 4.8, 8.8 Hz, 1 H), 7.45–7.40 (m, 2 H), 7.21 (d, J = 4.0 Hz, 1 H), 6.99 (t, J = 8.8 Hz, 2 H), 6.65–6.60 (m, 2 H), 4.08–4.02 (m, 2 H), 3.94 (d, J = 10.6 Hz, 1 H), 3.90–3.85 (m, 2 H), 3.35 (s, 3 H). *m/z*: 464.3.

**3-(5-((7aR)-6-(4-Fluorophenyl)-2-imino-3-methyl-4-oxooctahydro-1H-pyrrolo[3,4-d]pyrimidin-7a-yl)thiophen-3-yl)benzotrile (33).** Compound 33 was prepared from 23 in two steps following the general procedure C. <sup>1</sup>H NMR (400 MHz, CD<sub>3</sub>OD) δ 8.03 (m, 1H), 7.95 (m, 1H), 7.86 (m, 1H), 7.65 (m, 2H), 7.58 (t, J = 8.0 Hz, 1H), 6.98 (m, 2H), 6.63 (m, 2H), 4.07 (m, 2H), 3.91 (m, 3H), 3.34 (s, 3H). *m/z*: 446.2.

**3-(5-((7aR)-2-Imino-6-(3-isopropoxyphenyl)-3-methyl-4-oxooctahydro-1H-pyrrolo[3,4-d]pyrimidin-7a-yl)thiophen-3-yl)benzotrile (34).** Compound 34 was prepared from 23 in two steps following the general procedure C. <sup>1</sup>H NMR (400 MHz, CD<sub>3</sub>OD) δ 8.02 (m, 1H), 7.94 (m, 1H), 7.86 (m, 1H), 7.64 (m, 2H), 7.58 (t, J = 8.0 Hz, 1H), 7.11 (t, J = 8.0 Hz, 1H), 6.33 (m, 1H), 6.22 (m, 1H), 6.11 (m, 1H), 4.55 (m, 1H), 4.07 (m, 2H), 3.91 (m, 3H), 3.34 (s, 3H), 1.28 (d, J = 6.0 Hz, 6H). *m/z*: 486.3.

**(7aR)-2-Imino-6-(3-isopropoxyphenyl)-3-methyl-7a-(4-(5-(prop-1-yn-1-yl)pyridin-3-yl)thiophen-2-yl)hexahydro-1H-pyrrolo[3,4-d]pyrimidin-4(4aH)-one (35).** Compound 35 was prepared from 25 in two steps following the general procedure C. <sup>1</sup>H NMR (400 MHz, CD<sub>3</sub>OD) δ 8.87 (br s, 1H), 8.49 (s, 1H), 8.05 (s, 1H), 7.72 (s, 1H), 7.09 (t, J = 8 Hz, 1H), 6.32 (m, 1H), 6.23 (m, 1H), 6.16 (m, 1H), 4.56 (m, 1H), 4.04 (m, 2H), 3.99 (m, 3H), 3.33 (s, 3H), 2.12 (s, 3H), 1.28 (d, J = 6.0 Hz, 6H). *m/z*: 500.3.

**3-(5-((7aR)-2-Imino-3-methyl-4-oxo-6-(pyridin-2-yl)octahydro-1H-pyrrolo[3,4-d]pyrimidin-7a-yl)thiophen-3-yl)benzotrile (36).** Compound 36 was prepared from 23 in two steps following the general procedure D. <sup>1</sup>H NMR (400 MHz, CD<sub>3</sub>OD) δ 8.06 (m, 3H), 7.97 (m, 1H), 7.94 (m, 1H), 7.71 (m, 1H), 7.67 (m, 1H), 7.59 (t, J = 7.8 Hz, 1H), 7.15 (m, 1H), 7.06 (t, J = 7.0 Hz, 1H), 4.48 (d, J = 11.0 Hz, 1H), 4.24 (m, 4H), 3.35 (s, 3H). *m/z*: 429.2.

**3-(5-((7aR)-2-Imino-6-(3-methoxyphenyl)-3-methyl-4-oxooctahydro-1H-pyrrolo[3,4-d]pyrimidin-7a-yl)thiophen-3-yl)benzotrile (37).** Compound 37 was prepared from 23 in two steps following the general procedure D. <sup>1</sup>H NMR (400 MHz, CD<sub>3</sub>OD) δ 8.04 (m, 1H), 7.96 (m, 1H), 7.92 (m, 1H), 7.62 (m, 5H),



6.99 (m, 1H), 4.65 (d,  $J = 12$  Hz, 1H), 4.42 (m, 3H), 4.1 (t,  $J = 8.7$  Hz, 1H), 3.9 (s, 3H), 3.34 (s, 3H).  $m/z$ : 459.3.

**2-((7aR)-7a-(4-(3-Cyanophenyl)thiophen-2-yl)-2-imino-3-methyl-4-oxohexahydro-1H-pyrrolo[3,4-d]pyrimidin-6(2H)-yl)-nicotinonitrile (38).** Compound 38 was prepared from 23 in two steps following the general procedure D.  $^1\text{H}$  NMR (400 MHz,  $\text{CD}_3\text{OD}$ )  $\delta$  8.35 (m, 1H), 8.03 (m, 1H), 7.97 (m, 1H), 7.95 (m, 1H), 7.92 (m, 1H), 7.89 (m, 2H), 7.66 (m, 2H), 7.58 (m, 1H), 6.85 (m, 1H), 4.64 (d,  $J = 12$  Hz, 1H), 4.38 (m, 3H), 4.14 (t,  $J = 8.42$  Hz, 1H), 3.34 (s, 3H).  $m/z$ : 454.2.

**3-(5-((4aR,7aR)-6-(5-Fluoropyridin-2-yl)-2-imino-3-methyl-4-oxooctahydro-1H-pyrrolo[3,4-d]pyrimidin-7a-yl)thiophen-3-yl)benzotrile (39).** Compound 39 was prepared from 23 in two steps following the general procedure D.  $^1\text{H}$  NMR (400 MHz,  $\text{CD}_3\text{OD}$ )  $\delta$  8.08 (m, 1H), 8.03 (m, 1H), 7.95 (m, 1H), 7.88 (m, 1H), 7.65 (m, 2H), 7.60 (m, 2H), 6.63 (d,  $J = 9.0$  Hz, 1H), 4.32 (d,  $J = 11.0$  Hz, 1H), 4.12 (m, 3.0 Hz), 3.98 (m, 1H), 3.34 (s, 3H).  $m/z$ : 447.2.

**3-(5-((7aR)-2-Imino-6-(6-methoxypyridin-2-yl)-3-methyl-4-oxooctahydro-1H-pyrrolo[3,4-d]pyrimidin-7a-yl)thiophen-3-yl)benzotrile (40).** Compound 40 was prepared from 23 in two steps following the general procedure D.  $^1\text{H}$  NMR (400 MHz,  $\text{CD}_3\text{OD}$ )  $\delta$  8.04 (m, 1H), 7.97 (m, 1H), 7.91 (m, 1H), 7.76–7.65 (m, 3H), 7.59 (t,  $J = 7.6$  Hz, 1H), 6.33 (m, 2H), 4.4 (d,  $J = 11.7$  Hz, 1H), 4.13 (m, 4H), 3.97 (s, 3H), 3.35 (s, 3H).  $m/z$ : 459.3.

**3-(5-((7aR)-2-Imino-3-methyl-4-oxo-6-(6-(trifluoromethyl)pyridin-2-yl)octahydro-1H-pyrrolo[3,4-d]pyrimidin-7a-yl)thiophen-3-yl)benzotrile (41).** Compound 41 was prepared from 23 in two steps following the general procedure D.  $^1\text{H}$  NMR (400 MHz,  $\text{CD}_3\text{OD}$ )  $\delta$  8.04 (m, 1H), 7.96 (m, 1H), 7.88 (m, 1H), 7.74 (t,  $J = 8.0$  Hz, 1H), 7.66 (m, 2H), 7.58 (t,  $J = 8.0$  Hz, 1H), 7.05 (d,  $J = 7.3$  Hz, 1H), 6.80 (d,  $J = 7.3$  Hz, 1H), 4.42 (d,  $J = 12$  Hz, 1H), 4.15 (m, 3H), 4.02 (m, 1H), 3.34 (s, 3H).  $m/z$ : 497.3.

**3-(5-((7aR)-2-Imino-3-methyl-4-oxo-6-(pyrimidin-2-yl)octahydro-1H-pyrrolo[3,4-d]pyrimidin-7a-yl)thiophen-3-yl)benzotrile (42).** Compound 42 was prepared from 23 in two steps following the general procedure D.  $^1\text{H}$  NMR (400 MHz,  $\text{CD}_3\text{OD}$ )  $\delta$  8.59 (m, 2H), 8.04 (m, 1H), 7.97 (m, 1H), 7.93 (m, 1H), 7.71 (m, 1H), 7.67 (m, 1H), 7.59 (t,  $J = 7.8$  Hz, 1H), 7.0 (m, 1H), 4.63 (m, 1H), 4.31 (m, 4H), 3.35 (s, 3H).  $m/z$ : 430.2.

**3-(5-((7aR)-6-(5-Fluoropyrimidin-2-yl)-2-imino-3-methyl-4-oxooctahydro-1H-pyrrolo[3,4-d]pyrimidin-7a-yl)thiophen-3-yl)benzotrile (43).** Compound 43 was prepared from 23 in two steps following the general procedure D.  $^1\text{H}$  NMR (400 MHz,  $\text{CD}_3\text{OD}$ )  $\delta$  8.34 (m, 2H), 8.01 (m, 1H), 7.93 (m, 1H), 7.80 (m, 1H), 7.64 (m, 1H), 7.56 (m, 2H), 4.34 (d,  $J = 11.7$  Hz, 1H), 4.2–3.8 (m, 4H), 3.29 (s, 3H).  $m/z$ : 448.2.

**3-(5-((7aR)-6-(5-Chloropyrimidin-2-yl)-2-imino-3-methyl-4-oxooctahydro-1H-pyrrolo[3,4-d]pyrimidin-7a-yl)thiophen-3-yl)benzotrile (44).** Compound 44 was prepared from 23 in two steps following the general procedure D.  $^1\text{H}$  NMR (400 MHz,  $\text{CD}_3\text{OD}$ )  $\delta$  8.34 (m, 2H), 8.04 (m, 1H), 7.97 (m, 1H), 7.88 (m, 1H), 7.66 (m, 2H), 7.58 (t,  $J = 8.0$  Hz, 1H), 4.45 (d,  $J = 12.0$  Hz, 1H), 4.23–4.03 (m, 4H), 3.34 (s, 3H).  $m/z$ : 464.3.

**3-(5-((7aR)-2-Imino-3-methyl-6-(5-methylpyrimidin-2-yl)-4-oxooctahydro-1H-pyrrolo[3,4-d]pyrimidin-7a-yl)thiophen-3-yl)benzotrile (45).** Compound 45 was prepared from 23 in two steps following the general procedure D.  $^1\text{H}$  NMR (400 MHz,  $\text{CD}_3\text{OD}$ )  $\delta$  8.31 (m, 2H), 8.01 (m, 1H), 7.95 (m, 1H), 7.87 (m, 1H), 7.65 (m, 2H), 7.57 (t,  $J = 7.7$  Hz, 1H), 4.46 (d,  $J = 12.0$  Hz, 1H), 4.25–4.03 (m, 4H), 3.34 (s, 3H), 2.18 (s, 3H).  $m/z$ : 444.2.

**3-(5-((7aR)-6-(5-Fluoro-4-methoxypyrimidin-2-yl)-2-imino-3-methyl-4-oxooctahydro-1H-pyrrolo[3,4-d]pyrimidin-7a-yl)thiophen-3-yl)benzotrile (45).** Compound 45 was prepared from 27 in two steps following the general procedure D.  $^1\text{H}$  NMR (400 MHz,  $\text{CD}_3\text{OD}$ )  $\delta$  8.05 (m, 2H), 7.96 (m, 1H), 7.88 (m, 1H), 7.65 (m, 2H), 7.58 (t,  $J = 7.8$  Hz, 1H), 4.45 (m, 1H), 4.20–4.00 (m, 4H), 3.34 (s, 3H).  $m/z$ : 478.3.

## AUTHOR INFORMATION

### Corresponding Author

\*Phone: 732-594-3369. Fax: 732-594-1185. E-mail: mihirbaran.mandal@merck.com.

### Notes

The authors declare no competing financial interest.

## ACKNOWLEDGMENTS

We thank T.-M.Chan for his help in compound characterization, Drs. Jim Tata and Ann Weber for their strong support, and Dr. Eric Gilbert for helpful feedback on the manuscript. Use of the IMCA-CAT beamline 17-ID (or 17-BM) at the Advanced Photon Source was supported by the companies of the Industrial Macromolecular Crystallography Association through a contract with Hauptman-Woodward Medical Research Institute. Use of the Advanced Photon Source was supported by the U.S. Department of Energy, Office of Science, Office of Basic Energy Sciences, under Contract No. DE-AC02-06CH11357.

## ABBREVIATIONS USED

AUC, area under the curve; BACE,  $\beta$ -site APP-cleaving enzyme; AD, Alzheimer's disease;  $A\beta$ ,  $\beta$ -amyloid; SAR, structure–activity relationship; CNS, central nervous system; CSF, cerebrospinal fluid; Pgp, P-glycoprotein; HTS, high throughput screening; ER, efflux ratio; LE, ligand efficiency;  $K_d$ , dissociation constant; PK, pharmacokinetic; PD, pharmacodynamic; hERG, the human ether-à-go-go-related gene; CYP, cytochrome P450; hPXR, human pregnane X receptor; EDC, 1-ethyl-3-(3-dimethylaminopropyl) carbodiimide hydrochloride

## REFERENCES

- (1) (a) Tariot, P. N.; Federoff, H. J. Current Treatment for Alzheimer Disease and Future Prospects. *Alzheimer Dis. Assoc. Disord.* **2003**, *17*, S105–S113. (b) Nordberg, A. Mechanisms behind the neuroprotective actions of cholinesterase inhibitors in Alzheimer disease. *Alzheimer Dis. Assoc. Disord.* **2006**, *20*, S12–S18. (c) Bullock, R. Efficacy and safety of memantine in moderate-to-severe Alzheimer disease: the evidence to date. *Alzheimer Dis. Assoc. Disord.* **2006**, *20*, 23–29.
- (2) (a) Hardy, J.; Selkoe, D. J. The Amyloid hypothesis of Alzheimer's disease: progress and problems on the road to therapeutics. *Science* **2002**, *297*, 353–356. (b) Korszyn, A. D. The amyloid cascade hypothesis. *Alzheimer's Dementia* **2008**, *4*, 176–178. (c) Hardy, J. Has the amyloid cascade hypothesis for Alzheimer's been proved? *Curr. Alzheimer Res.* **2006**, *3*, 71–73. (d) Selkoe, D. Alzheimer's disease: genes, proteins, and therapy. *Physiol. Rev.* **2001**, *81*, 741–766. (e) Archer, H. A.; Edison, P.; Brooks, D. J.; Barnes, J.; Frost, C.; Yeatman, T. Amyloid load and cerebral atrophy in Alzheimer's disease: a  $^{11}\text{C}$ -BIP positron emission tomography study. *Ann. Neurol.* **2006**, *60*, 145–147.
- (3) (a) Haass, C.; Selkoe, D. J. Soluble protein oligomers in neurodegeneration: lessons from the Alzheimer's amyloid  $\beta$ -peptide. *Nature Rev. Mol. Cell Biol.* **2007**, *8*, 101–112. (b) Kaye, R.; Head, E.; Thompson, J. L.; McIntire, T. M.; Milton, S. C.; Cotman, C. W.; Glabe, C. G. Common structure of soluble amyloid oligomers implies common mechanism of pathogenesis. *Science* **2003**, *300*, 486–489. (c) Dahlgren, K. N.; Manelli, A. M.; Stine, W. B.; Baker, L. K.; Krafft, G. A.; LaDu, M. J. Oligomeric and fibrillar species of amyloid-beta peptides differentially affect neuronal viability. *J. Biol. Chem.* **2002**, *277*, 32046–32053. (d) Rodrigues, C. M.; Sola, S.; Brito, M. A.; Brondino, C. D.; Brites, D.; Moura, J. J. Amyloid beta-peptide disrupts mitochondrial membrane lipid and protein structure: protective role of tauroursodeoxycholate. *Biochem. Biophys. Res. Commun.* **2001**, *281*, 468–474. (e) Lambert, M. P.; Barlow, A. K.; Chromy, B. A.; Edwards,



C.; Freed, R.; Liosatos, M.; Morgan, T. E.; Rozovsky, I.; Trommer, B.; Viola, K. L.; Wals, P.; Zhang, C.; Finch, C. E.; Krafft, G. A.; Klein, W. L. Diffusible, nonfibrillar ligands derived from  $A\beta_{1-42}$  are potent central nervous system neurotoxins. *Proc. Natl. Acad. Sci. U. S. A.* **1998**, *95*, 6448–6453. (f) Kuo, Y. M.; Emmerling, M. R.; Vigo-Pelfrey, C.; Kasunic, T. C.; Kirkpatrick, J. B.; Murdoch, G. H.; Ball, M. J.; Røher, A. E. Water-soluble  $A\beta$  (N-40, N-42) oligomers in normal and Alzheimer disease brains. *J. Biol. Chem.* **1996**, *271*, 4077–4081.

(4) Schellenberg, G. D.; Montine, T. J. The genetics and neuropathology of Alzheimer's disease. *Acta Neuropathol.* **2012**, May 23.

(5) (a) Artavanis-Tsakonas, S.; Rand, M. D.; Lake, R. J. Notch signaling: cell fate control and signal bintegration in development. *Science* **1999**, *284*, 770–776. (b) Hüll, M.; Berger, M.; Heneka, M. Disease-modifying therapies in Alzheimer's disease. *Drug* **2006**, *66*, 2075–2093. (c) Siemers, E. R.; Quinn, J. F.; Kaye, J.; Farlow, M. R.; Porsteinsson, A.; Tariot, P.; Zoulnouni, P.; Galvin, J. E.; Holtzman, D. M.; Knopman, D. S.; Satterwhite, J.; Gonzales, C.; Dean, R. A.; May, P. C. Effects of a  $\gamma$ -secretase inhibitor in a randomized study of patients with Alzheimer disease. *Neurology* **2006**, *66*, 602–604. (d) Fleisher, A. S.; Raman, R.; Siemers, E. R.; Becerra, L.; Clark, C. M.; Dean, R. A.; Farlow, M. R.; Galvin, J. E.; Peskind, E. R.; Quinn, J. F.; Sherzai, A.; Sowell, B. B.; Aisen, P. S.; Thal, L. J. Phase 2 safety trial targeting amyloid  $\beta$  production with a  $\gamma$ -secretase inhibitor in Alzheimer disease. *Arch. Neurol.* **2008**, *65*, 1031–1038. (e) Siemers, E.; Skinner, M.; Dean, R. A.; Gonzales, C.; Satterwhite, J.; Farlow, M.; Ness, D.; May, P. C. Safety, tolerability, and changes in amyloid  $\beta$  concentrations after administration of a  $\gamma$ -secretase inhibitor in volunteers. *Clin. Neuropharmacol.* **2007**, *28*, 126–132. (f) Bateman, R. J.; Siemers, E. R.; Mawuenyega, K. G.; Wen, G.; Browning, K. R.; Sigurdson, W. C.; Yarasheski, K. E.; Friedrich, S. W.; DeMattos, R. B.; May, P. C.; Paul, S. M.; Holtzman, D. M. A  $\gamma$ -secretase inhibitor decreases amyloid- $\beta$  production in the central nervous system. *Ann. Neurol.* **2009**, *66*, 48–64. (g) Carlson, C.; Estergard, W.; Oh, J.; Suhy, J.; Jack, C. R., Jr.; Siemers, E.; Barakos, J. Prevalence of asymptomatic vasogenic edema in pretreatment Alzheimer's disease study cohorts from phase 3 trials of semagacestat and solanezumab. *Alzheimer's Dementia* **2011**, *7*, 396–401.

(6) (a) Hussain, I.; Powell, D.; Howlett, D. R.; Tew, D. G.; Meek, T. D.; Chapman, C.; Gloger, I. S.; Murphy, K. E.; Southan, C. D.; Ryan, D. M.; Smith, T. S.; Simmons, D. L.; Walsh, F. S.; Dingwall, C.; Christie, G. Identification of a novel aspartic protease (Asp 2) as beta-secretase. *Mol. Cell Neurosci.* **1999**, *14*, 419–427. (b) Sinha, S.; Anderson, J. P.; Barbour, R.; Basi, G. S.; Caccavello, R.; Davis, D.; Doan, M.; Dovey, H. F.; Frigon, N.; Hong, J.; Jacobson-Croak, K.; Jewett, N.; Keim, P.; Knops, J.; Lieberburg, I.; Power, M.; Tan, H.; Tatsuno, G.; Tung, J.; Schenk, D. Purification and cloning of amyloid precursor protein beta secretase from human brain. *Nature* **1999**, *402*, 537–540. (c) Vassar, R.; Bennett, B. D.; Babu-Khan, S.; Kahn, S.; Mendiaz, E. A.; Denis, P.; Teplow, D. B.; Ross, S.; Amarante, P.; Loeloff, R.; Luo, Y.; Fisher, S.; Fuller, J.; Edenson, S.; Lile, J.; Jarosinski, M. A.; Biere, A. L.; Curran, E.; Burgess, T.; Louis, J. C. Beta-secretase cleavage of Alzheimer's amyloid precursor protein by the transmembrane aspartic protease BACE. *Science* **1999**, *286*, 735–741. (d) Yan, R.; Bienkowski, M. J.; Shuck, M. E.; Miao, H.; Tory, M. C.; Pauley, A. M.; Brashier, J. R.; Stratman, N. C.; Mathews, W. R.; Buhl, A. E.; Carter, D. B.; Tomasselli, A. G.; Parodi, L. A.; Heinrich, R. L.; Gurney, M. E. Membrane-anchored aspartyl protease with Alzheimer's disease beta-secretase activity. *Nature* **1999**, *402*, 533–537.

(7) (a) Luo, Y.; Bolon, B.; Kahn, S.; Bennett, B. D.; Babu-Khan, S.; Denis, P.; Fan, W.; Kha, H.; Zhang, J.; Gong, Y.; Martin, L.; Louis, J. C.; Yan, Q.; Richards, W. G.; Citron, M.; Vassar, R. Mice deficient in BACE1, the Alzheimer's beta secretase, have normal phenotype and abolished beta-amyloid generation. *Nature Neurosci.* **2001**, *4*, 231–232. (b) Luo, Y.; Bolon, B.; Damore, M. A.; Fitzpatrick, D.; Liu, H.; Zhang, J.; Yan, Q.; Vassar, R.; Citron, M. BACE1 (beta secretase) knockout mice do not acquire compensatory gene expression changes or develop neural lesions over time. *Neurobiol. Dis.* **2003**, *14*, 81–88.

(8) (a) Willem, M.; Garratt, A. N.; Novak, B.; Citron, M.; Kaufmann, S.; Rittger, A.; DeStrooper, B.; Saftig, P.; Birchmeier, C.; Haass, C.

Control of Peripheral Nerve Myelination by the beta-Secretase BACE1. *Science* **2006**, *314*, 664–666. (b) Wang, H.; Song, L.; Laird, F.; Wong, P. C.; Lee, H.-K. BACE1 knock-outs display deficits in activity-dependent potentiation of synaptic transmission at mossy fiber to CA3 synapses in the hippocampus. *J. Neurosci.* **2008**, *28*, 8677–8681.

(9) Ohno, M.; Sametsky, E. A.; Younkin, L. H.; Oakley, H.; Younkin, S. G.; Citron, M.; Vassar, R.; Disterhoft, J. F. BACE1 deficiency rescues memory deficits and cholinergic dysfunction in a mouse model of Alzheimer's disease. *Neuron* **2004**, *41*, 27–33.

(10) McConlogue, L.; Buttini, M.; Anderson, J. P.; Brigham, E. F.; Chen, K. S.; Freedman, S. B.; Games, D.; Wood, K. J.; Lee, M.; Zeller, M.; Liu, W.; Motter, R.; Sinha, S. Partial reduction of BACE1 has dramatic effects on Alzheimer plaque and synaptic pathology in APP transgenic mice. *J. Biol. Chem.* **2007**, *282*, 8589–8595.

(11) (a) Mehellou, Y.; Clercq, E.-D. Twenty-six years of anti-HIV drug discovery: where do we stand and where do we go? *J. Med. Chem.* **2010**, *53*, 521–538. (b) Surleraux, D. L. N. G.; Tahri, A.; Verschuere, W. G.; Pille, G. M. E.; Kock, H. A.; Jonckers, T. H. M.; Peeters, A.; De Meyer, S.; Azijn, H.; Pauwels, R.; Bethune, M.-P.; King, N. M.; Prabujeyabalan, M.; Schiffer, C. A.; Wigerinck, P. B. T. P. Discovery and selection of TMC114, a next generation HIV-1 protease inhibitor. *J. Med. Chem.* **2005**, *48*, 1813–1822. (c) Dorsey, B. D.; McDonough, C.; McDaniel, S.; L.; Levin, R. B.; Newton, C. L.; Hoffman, J. M.; Darke, P. L.; Zugay-Murphy, J. A.; Emini, E. A.; Schleif, W. A.; Olsen, D. B.; Stahlhut, M. W.; Rutkowski, C. A.; Kuo, L. C.; Lin, J. H.; Chen, L.-W.; Michelson, R. S.; Holloway, M. K.; Huff, J. R.; Vacca, J. P. Identification of MK-944a: a second clinical candidate from the hydroxylaminepentanamide isostere series of HIV protease inhibitors. *J. Med. Chem.* **2000**, *43*, 3386–3399. (d) Kempf, D. J.; Sham, H. L.; Marsh, K. C.; Flentge, C. A.; Betebenner, D.; Green, B. E.; McDonald, E.; Vasavanonda, S.; Saldivar, A.; Wideburg, N. E.; Kati, W. M.; Ruiz, L.; Zhao, C.; Fino, L.; Patterson, J.; Molla, A.; Plattner, J. J.; Norbeck, D. W. Discovery of ritonavir, a potent inhibitor of HIV protease with high oral bioavailability and clinical efficacy. *J. Med. Chem.* **1998**, *41*, 602–617. (e) Bold, G.; Fässler, A.; Capraro, H. G.; Cozens, R.; Klimkait, T.; Lazdins, J.; Mestan, J.; Poncioni, B.; Rösel, J.; Stover, D.; Tintelnot-Blomley, M.; Acemoglu, F.; Beck, W.; Boss, E.; Eschbach, M.; Hürlimann, T.; Masso, E.; Roussel, S.; Ucci-Stoll, K.; Wyss, D.; Lang, M. New aza-dipeptide analogues as potent and orally absorbed HIV-1 protease inhibitors: candidates for clinical development. *J. Med. Chem.* **1998**, *41*, 3387–3401. (f) Kim, E. E.; Baker, C. T.; Dwyer, M. D.; Murcko, M. A.; Rao, B. G.; Tung, R. D.; Navia, M. A. Crystal structure of HIV-1 protease in complex with VX-478, a potent and orally bioavailable inhibitor of the enzyme. *J. Am. Chem. Soc.* **1995**, *117*, 1181–1182. (g) Dorsey, B. D.; Levin, R. B.; McDaniel, S. L.; Vacca, J. P.; Guare, J. P.; Darke, P. L.; Zugay, J. A.; Emini, E. A.; Schleif, W. A.; Quintero, J. A.; Lin, J. H.; Chen, W.; Holloway, M. K.; Fitzgerald, P. M. D.; Axel, M. G.; Ostovic, D.; Anderson, P. S.; Huff, J. R. L-735,524: the design of a potent and orally bioavailable HIV protease inhibitor. *J. Med. Chem.* **1994**, *37*, 3443–3451.

(12) (a) Webb, R. L.; Schiering, N.; Sedrani, R.; Maibaum, J. Direct renin inhibitors as a new therapy for hypertension. *J. Med. Chem.* **2010**, *53*, 7490–7520. (b) Maibaum, J.; Stutz, S.; Göschke, R.; Rigollier, P.; Yamaguchi, Y.; Cumin, F.; Rahuel, J.; Baum, H. P.; Cohen, N. C.; Schnell, C. R.; Fuhrer, W.; Grütter, M. G.; Schilling, W.; Wood, J. M. Structural modification of the P20 position of 2,7-dialkyl-substituted 5(S) amino-4(S)-hydroxy-8-phenyl-octanecarboxamides: the discovery of aliskiren, a potent nonpeptide human renin inhibitor active after once daily dosing in marmosets. *J. Med. Chem.* **2007**, *50*, 4832–4844.

(13) Ghosh, A. K.; Shin, D.; Downs, D.; Koelsch, G.; Lin, X.; Ermolieff, J.; Tang, J. Design of potent inhibitors for human brain memapsin 2 ( $\beta$ -secretase). *J. Am. Chem. Soc.* **2000**, *122*, 3522–3523.

(14) Hom, R. K.; Fang, L. R.; Mamo, S.; Tung, J. S.; Guinn, A. C.; Walker, D. E.; Davis, D. L.; Gailunas, A. F.; Thorsett, E. D.; Sinha, S.; Knops, J. E.; Jewett, N. E.; Anderson, J. P.; John, V. Design and synthesis of statin-based cell-permeable peptidomimetic inhibitors of human  $\beta$ -secretase. *J. Med. Chem.* **2003**, *46*, 1799–1802.

- (15) Hom, R. K.; Gailunas, A. F.; Mamo, S.; Fang, L. Y.; Tung, J. S.; Walker, D. E.; Davis, D.; Thorsett, E. D.; Jewett, N. E.; Moon, J. B.; John, V. Design and synthesis of hydroxyethylene-based peptidomimetic inhibitors of human  $\beta$ -secretase. *J. Med. Chem.* **2004**, *47*, 158–164.
- (16) Maillard, M. C.; Hom, R. K.; Benson, T. E.; Moon, J. B.; Mamo, S.; Bienkowski, M.; Tomasselli, A. G.; Woods, D. D.; Prince, D. B.; Paddock, D. J.; Emmons, T. L.; Tucker, J. A.; Dappen, M. S.; Brogley, L.; Thorsett, E. D.; Jewett, N.; Sinha, S.; John, V. Design synthesis, and crystal structure of hydroxyethyl secondary amine-based peptidomimetic inhibitors of human  $\beta$ -secretase. *J. Med. Chem.* **2007**, *50*, 776–781.
- (17) (a) Iserloh, U.; Wu, Y.; Cumming, J. N.; Pan, J.; Wang, L. Y.; Stamford, A. W.; Kennedy, M. E.; Kuvelkar, R.; Chen, X.; Parker, E. M.; Strickland, C.; Voigt, J. Potent pyrrolidine and piperidine-based BACE-1 inhibitors. *Bioorg. Med. Chem. Lett.* **2008**, *18*, 414–417. (b) Iserloh, U.; Pan, J.; Stamford, A. W.; Kennedy, M. E.; Zhang, Q.; Zhang, L.; Parker, E. M.; McHugh, N. A.; Favreau, L.; Strickland, C.; Voigt, J. Discovery of an orally efficacious 4-phenoxy-pyrrolidine-based BACE-1 inhibitor. *Bioorg. Med. Chem. Lett.* **2008**, *18*, 418–422. (c) Cumming, J. N.; Le, T. X.; Babu, S.; Carroll, C.; Chen, X.; Favreau, L.; Gaspari, P.; Guo, T.; Hobbs, D. W.; Huang, Y.; Iserloh, U.; Kennedy, M. E.; Kuvelkar, R.; Li, G.; Lowrie, J.; McHugh, N. A.; Ozgur, L.; Pan, J.; Parker, E. M.; Saionz, K.; Stamford, A. W.; Strickland, C.; Tadesse, D.; Voigt, J.; Wang, L.; Wu, Y.; Zhang, L.; Zhang, Q. Rational design of novel potent piperazinone and imidazolidinone BACE1 inhibitors. *Bioorg. Med. Chem. Lett.* **2008**, *18*, 3236–3241.
- (18) (a) Wang, Y.-S.; Strickland, C.; Voigt, J. H.; Kennedy, M. E.; Beyer, B. M.; Senior, M. M.; Smith, E. M.; Nechuta, T. L.; Madison, V. S.; Czarniecki, M.; McKittrick, B. A.; Stamford, A. W.; Parker, E. M.; Hunter, J. C.; Greenlee, W. J.; Wyss, D. F. Application of fragment-based NMR screening, X-ray crystallography, structure-based design, and focused chemical library design to identify novel  $\mu$ M leads for the development of nM BACE-1 ( $\beta$ -site APP cleaving enzyme 1) inhibitors. *J. Med. Chem.* **2010**, *53*, 942–950. (b) Zhu, Z.; Sun, Z.-Y.; Ye, Y.; Voigt, J.; Strickland, C.; Smith, E. M.; Cumming, J.; Wang, L.; Wong, J.; Wang, Y.-S.; Wyss, D. F.; Chen, X.; Kuvelkar, R.; Kennedy, M. E.; Favreau, L.; Parker, E.; McKittrick, B. A.; Stamford, A.; Czarniecki, M.; Greenlee, W.; Hunter, J. C. Discovery of cyclic acylguanidines as highly potent and selective  $\beta$ -site amyloid cleaving enzyme (BACE) inhibitors. Part I: inhibitor design and validation. *J. Med. Chem.* **2010**, *53*, 951–965.
- (19) (a) Malamas, M. S.; Erdei, J.; Gunawan, I.; Turner, J.; Hu, Y.; Wagner, E.; Fan, K.; Chopra, R.; Olland, A.; Bard, J.; Jacobsen, S.; Magolda, R. L.; Pangalos, M.; Robichaud, A. J. Design and synthesis of 5,5'-disubstituted aminohydantoin as potent and selective human  $\beta$ -secretase (BACE1) inhibitors. *J. Med. Chem.* **2010**, *53*, 1146–1158. (b) Malamas, M. S.; Erdei, J.; Gunawan, I.; Barnes, K.; Johnson, M.; Hui, Y.; Turner, J.; Hu, Y.; Wagner, E.; Fan, K.; Olland, A.; Bard, J.; Robichaud, A. J. Aminoimidazoles as potent and selective human  $\beta$ -secretase (BACE1) inhibitors. *J. Med. Chem.* **2009**, *52*, 6314–6323. (c) Barrow, J. C.; Stauffer, S. R.; Rittle, K. E.; Ngo, P. L.; Yang, Z.; Selnick, H. G.; Graham, S. L.; Munshi, S.; McGaughey, G. B.; Holloway, M. K.; Simon, A. J.; Price, E. A.; Sankaranarayanan, S.; Colussi, D.; Tugusheva, K.; Lai, M.-T.; Espeseth, A. S.; Xu, M.; Huang, Q.; Wolfe, A.; Pietrak, B.; Zuck, P.; Levorse, D. A.; Hazuda, D.; Vacca, J. P. Discovery and X-ray crystallographic analysis of a spiro-piperidine iminohydantoin inhibitor of  $\beta$ -secretase. *J. Med. Chem.* **2008**, *51*, 6259–6262. (d) Cole, D. C.; Manas, E. S.; Stock, J. R.; Condon, J. S.; Jennings, L. D.; Aulabaugh, A.; Chopra, R.; Cowling, R.; Ellingboe, J. W.; Fan, K. Y.; Harrison, B. L.; Hu, Y.; Jacobsen, S.; Jin, G.; Lin, L.; Lovering, F. E.; Malamas, M. S.; Stahl, M. L.; Strand, J.; Sukhdeo, M. N.; Svenson, K.; Turner, M. J.; Wagner, E.; Wu, J.; Zhou, P.; Bard, J. Acylguanidines as small-molecule  $\beta$ -secretase inhibitors. *J. Med. Chem.* **2006**, *49*, 6158–6161. (e) Baxter, E. W.; Conway, K. A.; Kennis, L.; Bischoff, F.; Mercken, M. H.; De Winter, H. L.; Reynolds, C. H.; Tounge, B. A.; Luo, C.; Scott, M. K.; Huang, Y.; Braeken, M.; Pieters, S. M. A.; Berthelot, D. J. C.; Masure, S.; Bruinzeel, W. D.; Jordan, A. D.; Parker, M. H.; Boyd, R. E.; Qu, J.; Alexander, R. S.; Brennehan, D. E.; Reitz, A. B. 2-Amino-3,4 dihydroquinazolines as inhibitors of BACE-1 ( $\beta$ -Site APP cleaving enzyme): use of structure based design to convert a micromolar hit into a nanomolar lead. *J. Med. Chem.* **2007**, *50*, 4162–4264. (f) Murray, C. W.; Callaghan, O.; Chessari, G.; Cleasby, A.; Congreve, M.; Frederickson, M.; Hartshorn, M. J.; McMenamin, R.; Patel, S.; Wallis, N. Application of fragment screening by X-ray crystallography to  $\beta$ -secretase. *J. Med. Chem.* **2007**, *50*, 1116–1123. (g) Congreve, M.; Aharon, D.; Albert, J.; Callaghan, O.; Campbell, J.; Carr, R. A. E.; Chessari, G.; Cowan, S.; Edwards, P. D.; Frederickson, M.; McMenamin, R.; Murray, C. W.; Patel, S.; Wallis, N. Application of fragment screening by X-ray crystallography to the discovery of aminopyridines as inhibitors of  $\beta$ -secretase. *J. Med. Chem.* **2007**, *50*, 1124–1132. (h) Geschwindner, S.; Olsson, L.-L.; Albert, J. S.; Deinum, J.; Edwards, P. D.; Beer, T.-D.; Folmer, R. H. A. Discovery of a novel warhead against  $\beta$ -secretase through fragment-based lead generation. *J. Med. Chem.* **2007**, *50*, 5903–5911. (i) Edwards, P. D.; Albert, J. S.; Sylvester, M.; Aharon, D.; Andisik, D.; Callaghan, O.; Campbell, J. B.; Carr, R. A.; Chessari, G.; Congreve, M.; Frederickson, M.; Folmer, R. H. A.; Geschwindner, S.; Koether, G.; Kolmodin, K.; Krumrine, J.; Mauger, R. C.; Murray, C. W.; Olsson, L.-L.; Patel, S.; Spear, N.; Tian, G. Application of fragment-based lead generation to the discovery of novel, cyclic amidine  $\beta$ -secretase inhibitors with nanomolar potency, cellular activity, and high ligand efficiency. *J. Med. Chem.* **2007**, *50*, 5912–5925. (j) Cheng, Y.; Judd, T. C.; Bartberger, M. D.; Brown, J.; Chen, K.; Freneau, R. T., Jr.; Hickman, D.; Hitchcock, S. A.; Jordan, B.; Li, V.; Lopez, P.; Louie, S. W.; Luo, Y.; Michelsen, K.; Nixey, T.; Powers, T. S.; Rattan, C.; Sickmier, E. A.; Jean, D. J., Jr.; Wahl, R. C.; Wen, P. H.; Wood, S. From fragment screening to in vivo efficacy: optimization of a series of 2-aminoquinolines as potent inhibitors of beta-site amyloid precursor protein cleaving enzyme 1 (BACE1). *J. Med. Chem.* **2011**, *54*, 5836–5857.
- (20) Cumming, J. N.; Smith, E. M.; Wang, L.; Misiaszek, J.; Durkin, J.; Pan, J.; Iserloh, U.; Wu, Y.; Zhu, Z.; Strickland, C.; Voigt, J.; Chen, X.; Kennedy, M. E.; Kuvelkar, R.; Hyde, L. A.; Cox, K.; Favreau, L.; Czarniecki, M. F.; Greenlee, W. J.; McKittrick, B. A.; Parker, E. M.; Stamford, A. W. Structure based design of iminohydantoin BACE1 inhibitors: identification of an orally available, centrally active BACE1 inhibitor. *Bioorg. Med. Chem. Lett.* **2012**, *22*, 2444–2449.
- (21) Stamford, A. W.; Scott, J. D.; Li, S. W.; Babu, S.; Tadesse, D.; Hunter, R.; Wu, Y.; Misiaszek, J.; Cumming, J. N.; Gilbert, E. J.; Huang, C.; McKittrick, B. A.; Hong, J.; Guo, T.; Zhu, Z.; Strickland, C.; Orth, P.; Voigt, J. H.; Kennedy, M. E.; Chen, X.; Kuvelkar, R.; Hodgson, R.; Hyde, L. A.; Cox, K.; Favreau, L.; Parker, E. M.; Greenlee, W. J. Discovery of an orally available, brain penetrant BACE1 inhibitor that affords robust CNS A $\beta$  reduction. *ACS Med. Chem. Lett.* **2012**, DOI: 10.1021/ml3001165.
- (22) Dean, W. D.; Blum, D. M. Condensation of arylacetonitriles with glyoxylic acid. Facile synthesis of arylmaleic acid derivatives. *J. Org. Chem.* **1993**, *58*, 7916–7917.
- (23) Lam, P. Y. S.; Clark, C. G.; Saubern, S.; Adams, J.; Winters, M. P.; Chan, D. M. T.; Combs, A. New aryl/heteroaryl C–N bond cross-coupling reactions via arylboronic acid/cupric acetate arylation. *Tetrahedron Lett.* **1998**, *39*, 2941–2944.
- (24) Wolfe, J. P.; Buchwald, S. L. Scope and limitations of the Pd/BINAP catalyzed amination of aryl bromides. *J. Org. Chem.* **2000**, *65*, 1144–1157.
- (25) Korfmacher, W. A.; Cox, K. A.; Ng, K. J.; Veals, J.; Hsien, Y.; Wainhaus, S.; Broske, L.; Prelusky, D.; Nomeir, A.; White, R. E. Cassette-accelerated rapid rat screen: a systematic procedure for the doing and liquid chromatography/atmospheric pressure ionization tandem mass spectrometric analysis of new chemical entities as part of new drug discovery. *Rapid Commun. Mass. Spectrom.* **2001**, *15*, 335–340.
- (26) (a) Rubas, W.; Jezyk, N.; Grass, G. M. Comparison of the permeability characteristics of a human colonic epithelial (Caco-2) cell line to colon of rabbit, monkey, and dog intestine and human drug absorption. *Pharm. Res.* **1993**, *10*, 113–118. (b) Makhey, V. D.; Guo,

A.; Norris, D. A.; Hu, P.; Yan, J.; Sinko, P. J. Characterization of the regional intestinal kinetics of drug efflux in rat and human intestine and in Caco-2 cells. *Pharm. Res.* **1998**, *15*, 1160–1167.

(27) (a) Didziapetris, R.; Japertas, P.; Avdeef, A.; Petrauskas, A. Classification Analysis of P Glycoprotein Substrate Specificity. *J. Drug Targeting* **2003**, *11*, 391. (b) Lu, K.; Jiang, Y.; Chen, B.; Eldemenky, E. M.; Ma, G.; Packiarajan, M.; Chandrasena, G.; White, A. D.; Jones, K. A.; Li, B.; Hong, S.-P. Strategies to lower the P-gp efflux liability in a series of potent indole azetidines MCHR1 antagonists. *Bioorg. Med. Chem. Lett.* **2011**, *21*, 5310–5314.

(28) Chein, R.-J.; Corey, E. J. Strong conformational preferences of heteroaromatic ethers and electron pair repulsion. *Org. Lett.* **2010**, *12*, 132–135.

(29) The free drug level in brain was estimated by applying the measured rat plasma free fraction to the total 6 h brain concentration from a rat 10 mg/kg PO PK experiment.

(30) *Schrödinger Modeling Software*; Schrödinger, LLC: 120 West 45th Street, New York, NY 10036.